

Supporting Information (Pages: S1-S49)

Six-coordinate $[\text{Co}^{\text{III}}(\text{L})_2]^z$ ($z = 1-, 0, 1+$) complexes of an azo-appended *o*-aminophenolate in amidate(2-) and iminosemiquinonate π -radical (1-) redox-levels: existence of valence-tautomerism

Amit Rajput, Anuj Kumar Sharma, Suman K. Barman, Francesc Lloret and Rabindranath Mukherjee*

Figures

Fig. S1 ESI-MS spectrum of $[\text{Co}(\text{L}^1)_2]$ **1**.

Fig. S2 IR spectrum of $[\text{Co}(\text{L}^1)_2]$ **1**.

Fig. S3 CVgram (100 mV/s) of one-electron oxidized 1.0 mM solution of $[\text{Co}(\text{L}^1)_2]$ **1**.

Fig. S4 CVgram (100 mV/s) of one-electron reduced 1.0 mM solution of $[\text{Co}(\text{L}^1)_2]$ **1**, $[\mathbf{1}]^{1-}$ species.

Fig. S5 ESI-MS of **2**.

Fig. S6 ESI-MS of **3**.

Fig. S7 CVgram (100 mV/s) of 1.0 mM solution of **2**.

Fig. S8 CVgram (100 mV/s) of 1.0 mM solution of **3**.

Fig. S9 IR spectrum of $[\text{Co}(\text{L}^1)_2][\text{PF}_6] \cdot 2\text{CH}_2\text{Cl}_2$ **2**.

Fig. S10 IR spectrum of $[\text{Co}^{\text{III}}(\eta^5\text{-C}_5\text{H}_5)_2][\text{Co}(\text{L}^1)_2]\text{MeCN}$ **3**.

Fig. S11 ^1H NMR spectrum (400 MHz, CDCl_3) of $[\text{Co}(\text{L}^1)_2]$ **1** at 298 K.

Fig. S12 Variable Temperature (VT) ^1H NMR spectrum (400 MHz, CDCl_3) of $[\text{Co}(\text{L}^1)_2]$ **1**.

Fig. S13 ^1H NMR spectrum (400 MHz, CDCl_3) of $[\text{Co}(\text{L}^1)_2][\text{PF}_6] \cdot 2\text{CH}_2\text{Cl}_2$ **2** at 298 K.

Fig. S14 Variable Temperature (VT) ^1H NMR spectrum (400 MHz, CDCl_3) of $[\text{Co}(\text{L}^1)_2][\text{PF}_6] \cdot 2\text{CH}_2\text{Cl}_2$ **2**.

Fig. S15 ^{13}C NMR spectrum (400 MHz, CDCl_3) of $[\text{Co}(\text{L}^1)_2][\text{PF}_6] \cdot 2\text{CH}_2\text{Cl}_2$ **2** at 298 K.

Fig. S16 2D HMQC (Heteronuclear Multiple Quantum Coherence) of (400 MHz, CDCl_3) $[\text{Co}(\text{L}^1)_2][\text{PF}_6] \cdot 2\text{CH}_2\text{Cl}_2$ **2**.

Fig. S17 ^1H NMR spectrum (400 MHz, CDCl_3) of $[\text{Co}^{\text{III}}(\eta^5\text{-C}_5\text{H}_5)_2][\text{Co}(\text{L}^1)_2]$ **3** 298 K.

Fig. S18 Variable Temperature (VT) ^1H NMR spectrum (400 MHz, CDCl_3) of $[\text{Co}^{\text{III}}(\eta^5\text{-C}_5\text{H}_5)_2][\text{Co}(\text{L}^1)_2]$ **3**.

Fig. S19 ^{13}C NMR spectrum (400 MHz, CDCl_3) of $[\text{Co}^{\text{III}}(\eta^5\text{-C}_5\text{H}_5)_2][\text{Co}(\text{L}^1)_2]$ **3** 298 K.

Fig. S20. Optimized-structure for $[\mathbf{1}]^{1-}$, where no spin-population is found.

Fig. S21 X-band EPR spectra recorded for $[\text{Co}^{\text{III}}(\eta^5\text{-C}_5\text{H}_5)_2][\text{Co}(\text{L}^1)_2]\text{MeCN}$ **3** as solid (298 K).

Fig. S22 UV-Vis-NIR spectra of **1-3** in CH_2Cl_2 .

Fig. S23 Absorption spectral measurements on ligand in neutral, dianionic and radical-anion forms recorded in CH_2Cl_2

Fig. S24 TD-DFT-calculated electronic spectra of **1**, $[\mathbf{1}]^{1+}$ and $[\mathbf{1}]^{1-}$.

Fig. S25. Representative molecular-orbitals involved in TD-DFT of **1**.

Fig. S26 Representative molecular orbitals involved in TD-DFT of $[\mathbf{1}]^{1+}$.

Fig. S27 Representative molecular orbitals involved in TD-DFT of $[\mathbf{1}]^{1-}$.

Tables

Table S1. Data collection and structure refinement parameters for $[\text{Co}(\text{L}^1)_2]$ **1**, $[\text{Co}^{\text{III}}(\text{L}^1)_2][\text{PF}_6] \cdot 2\text{CH}_2\text{Cl}_2$ **2**, and $[\text{Co}^{\text{III}}(\eta^5\text{-C}_5\text{H}_5)_2][\text{Co}(\text{L}^1)_2] \cdot \text{MeCN}$ **3**.

Table S2. Comparison of X-ray determined experimental bond lengths with the calculated bond lengths from metrical oxidation state MOS (in parentheses) of $[\text{Fe}(\text{L}^1)_2]$ and $[\text{Fe}(\text{L}^1)_2]^+$.

Table S3. DFT-optimized cartesian coordinates of **1**.

Table S4. DFT-optimized coordinates of $[\mathbf{1}]^{1+}$.

Table S5. DFT-optimized coordinates of $[\mathbf{1}]^{1-}$.

Table S6. X-ray structural and DFT-optimized (in parentheses) bond lengths of **1**, $[\mathbf{1}]^{1+}$ and $[\mathbf{1}]^{1-}$.

Table S7. TD-DFT-calculated electronic transitions of **1**.

Table S8. TD-DFT-calculated electronic transitions of $[\mathbf{1}]^{1+}$.

Table S9. TD-DFT-calculated electronic transitions of $[\mathbf{1}]^{1-}$.

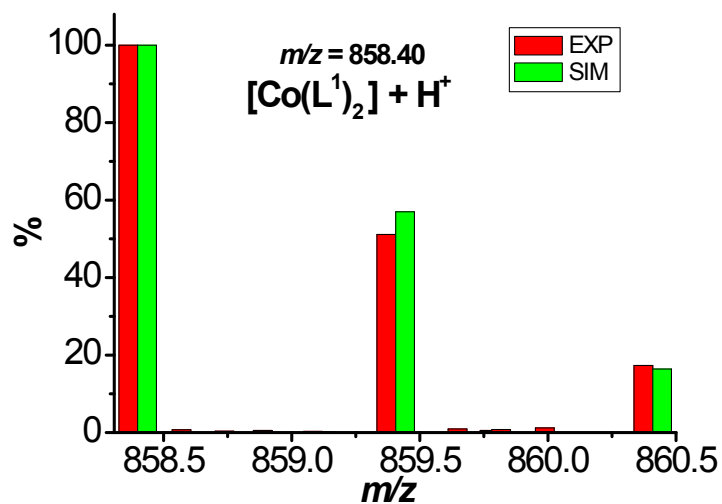


Fig. S1. Positive-ion ESI-MS spectrum of **1** $\{[\text{Co}(\text{L}^1)_2] + \text{H}^+\}$.

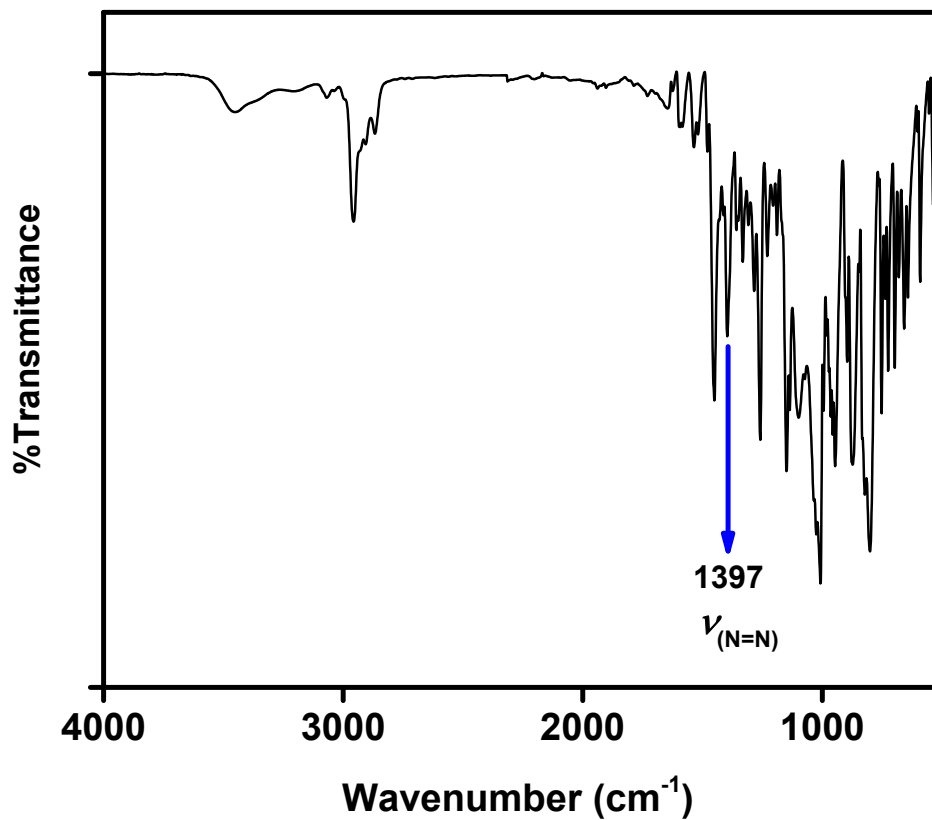


Fig. S2 IR spectrum of $[\text{Co}(\text{L}^1)_2]$ **1**.

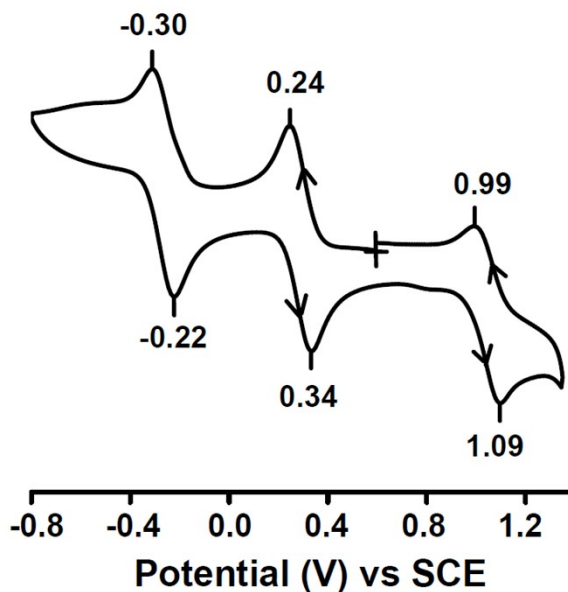


Fig. S3 CVgram (100 mV/s) of coulometrically-generated $1e^-$ oxidized 1.0 mM solution of $[\text{Co}(\text{L}^1)_2]$ **1** in CH_2Cl_2 (0.1 M in TBAP) at a platinum working electrode.

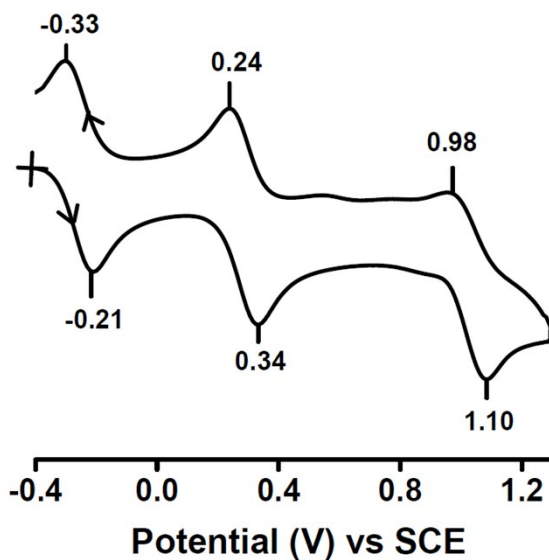


Fig. S4 CVgram (100 mV/s) of coulometrically-generated $1e^-$ reduced 1.0 mM solution of $[\text{Co}(\text{L}^1)_2]$ **1** in CH_2Cl_2 (0.1 M in TBAP) at a platinum working electrode.

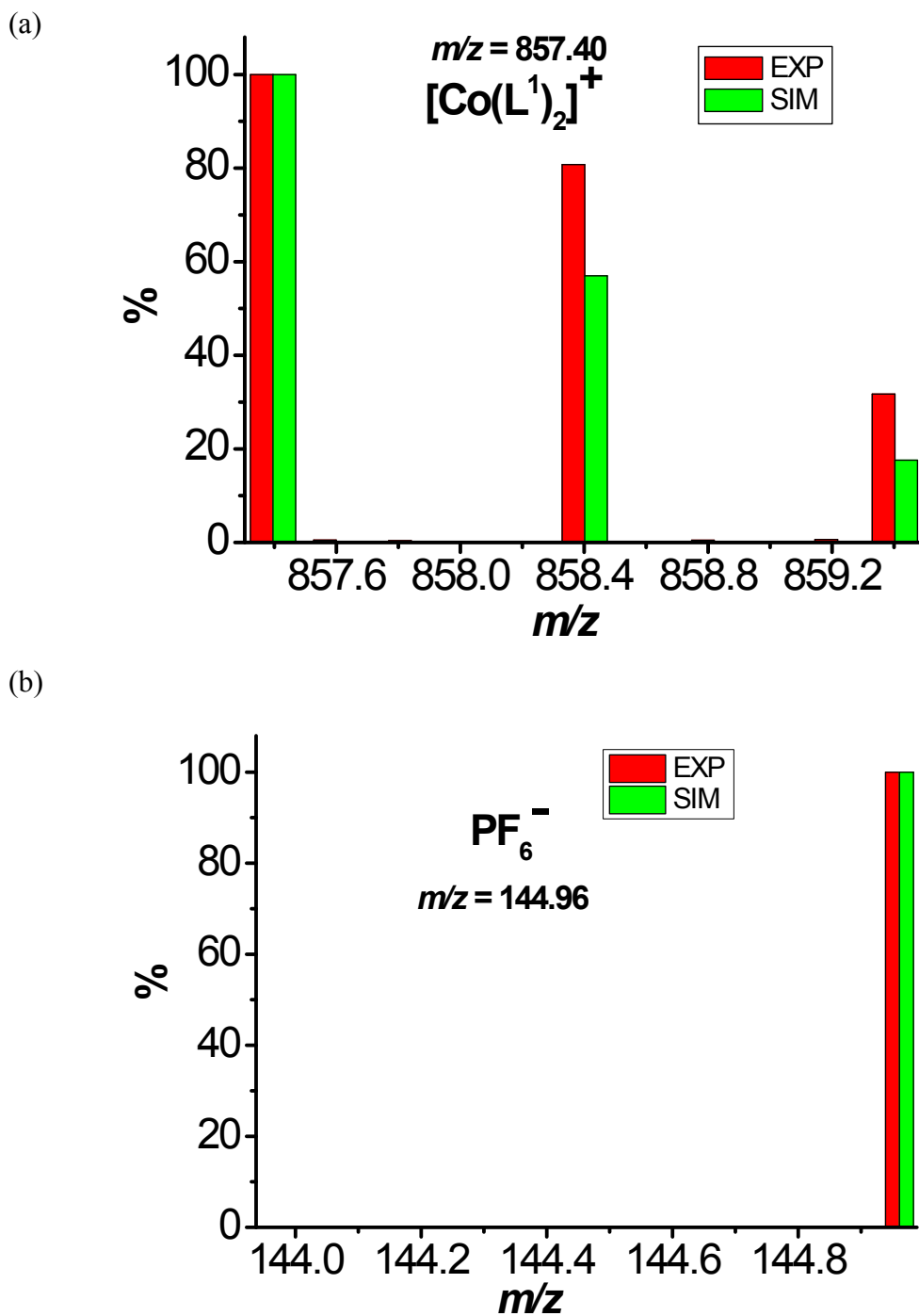


Fig. S5 (a) Positive ESI-MS spectrum of $[\text{Co}(\text{L}^1)_2]^+$ (cationic part) and (b) negative ESI-MS Spectrum of PF_6^- (anionic part) of $[\text{Co}^{\text{III}}(\text{L}^1)_2][\text{PF}_6] \cdot 2\text{CH}_2\text{Cl}_2$ **2**.

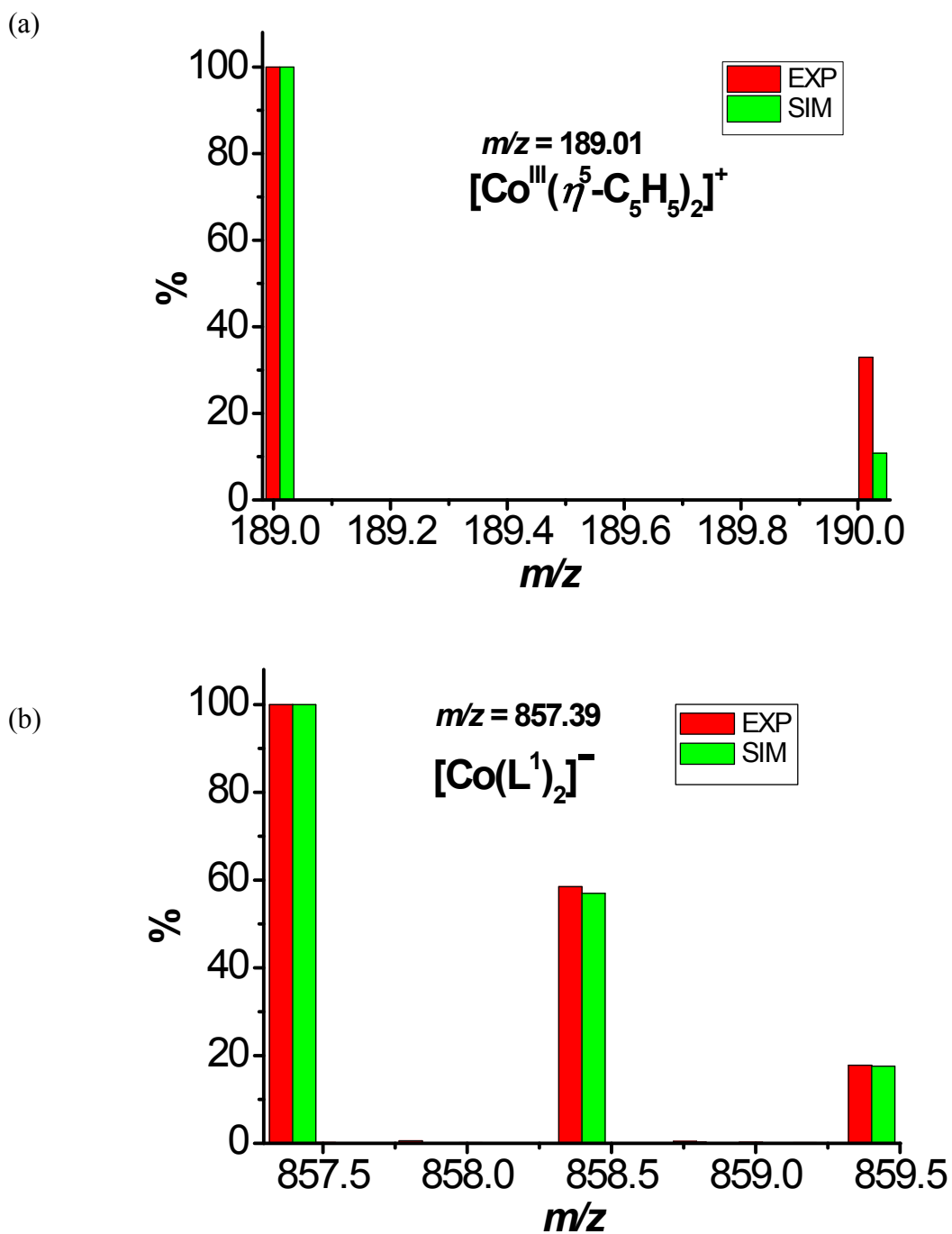


Fig. S6 (a) Positive ESI-MS spectrum of $[\text{Co}^{\text{III}}(\eta^5\text{-C}_5\text{H}_5)_2]^+$ (cationic part) and (b) negative ESI-MS spectrum of $[\text{Co}(\text{L}^1)_2]^-$ (anionic part) of $[\text{Co}^{\text{III}}(\eta^5\text{-C}_5\text{H}_5)_2]^-[\text{Co}(\text{L}^1)_2]\cdot\text{CH}_3\text{CN}$ 3.

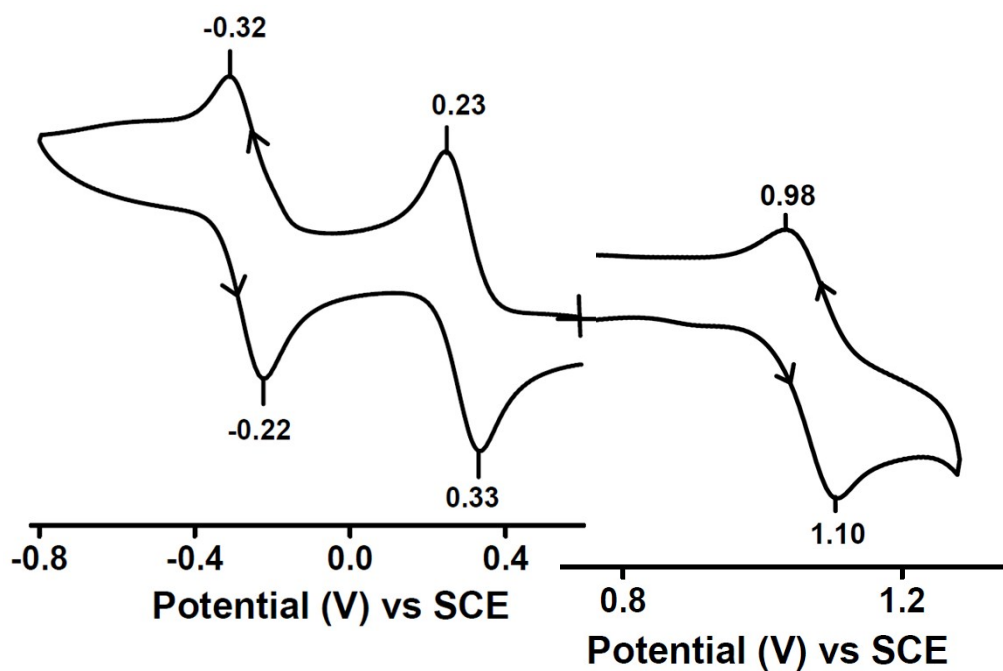


Fig. S7 Cyclic voltammogram (100 mV/s) of a 1.0 mM solution of $[\text{Co}(\text{L}^1)_2][\text{PF}_6] \cdot 2\text{CH}_2\text{Cl}_2$ **2** in CH_2Cl_2 (0.1 M in TBAP) at a platinum working electrode.

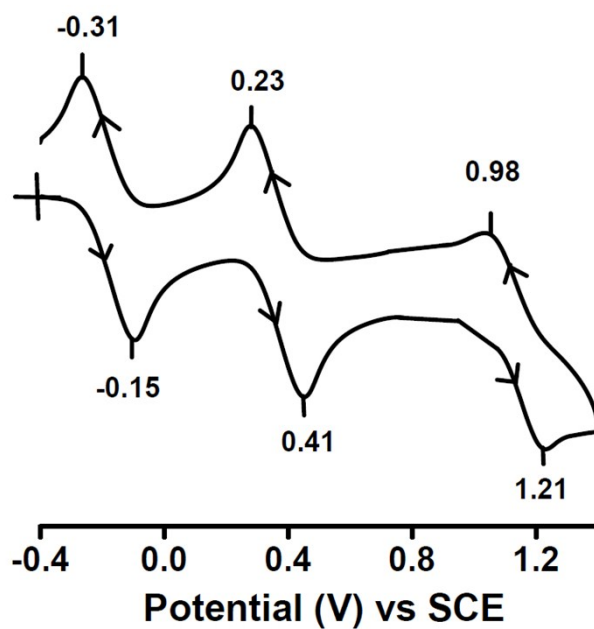


Fig. S8 Cyclic voltammogram (100 mV/s) of a 1.0 mM solution of $[\text{Co}^{\text{III}}(\eta^5\text{-C}_5\text{H}_5)_2][\text{Co}(\text{L}^1)_2] \cdot \text{CH}_3\text{CN}$ **3** in CH_2Cl_2 (0.1 M in TBAP) at a platinum working electrode.

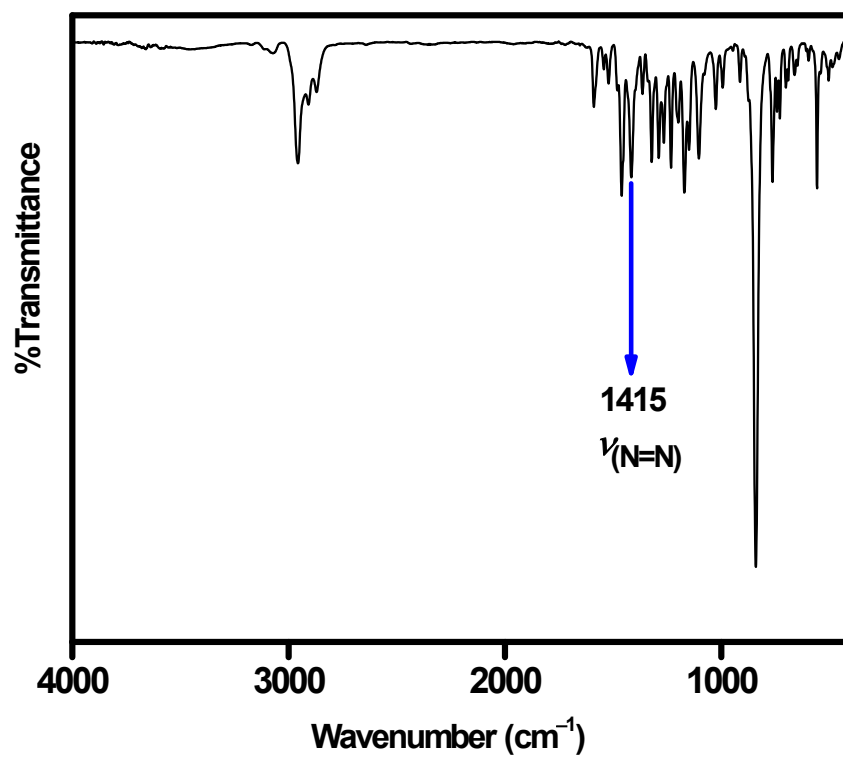


Fig. S9 IR spectrum of [Co(L¹)₂][PF₆] \cdot 2CH₂Cl₂ 2.

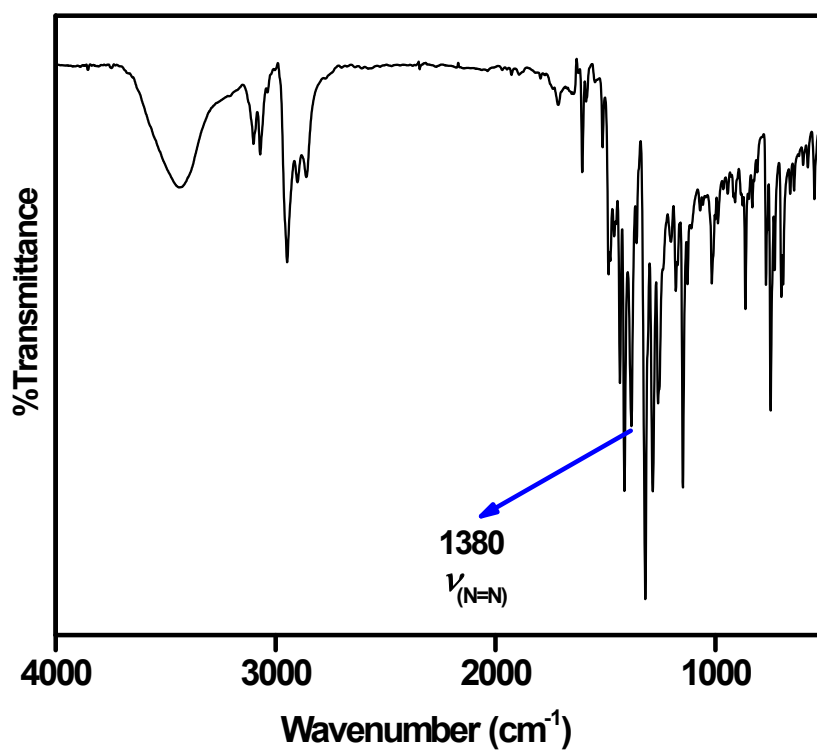


Fig. S10 IR spectrum of [Co^{III}(η^5 -C₅H₅)₂][Co(L¹)₂]MeCN 3.

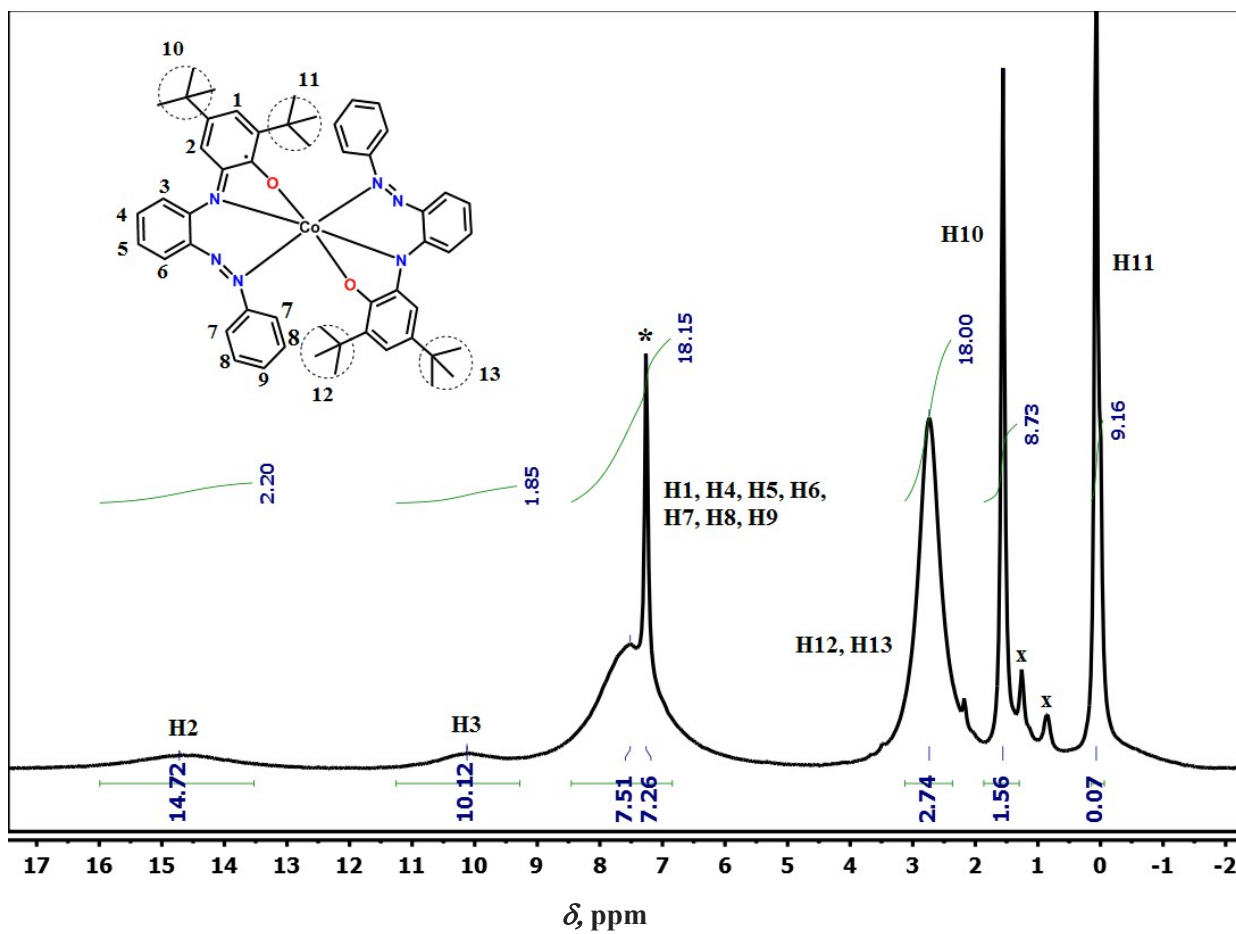


Fig. S11 ^1H NMR spectrum (400 MHz, CDCl_3) of $[\text{Co}(\text{L}^1)_2]$ **1** at 298 K. Peak denoted by * and x are due to CHCl_3 and solvent impurity, respectively.

downfield shift



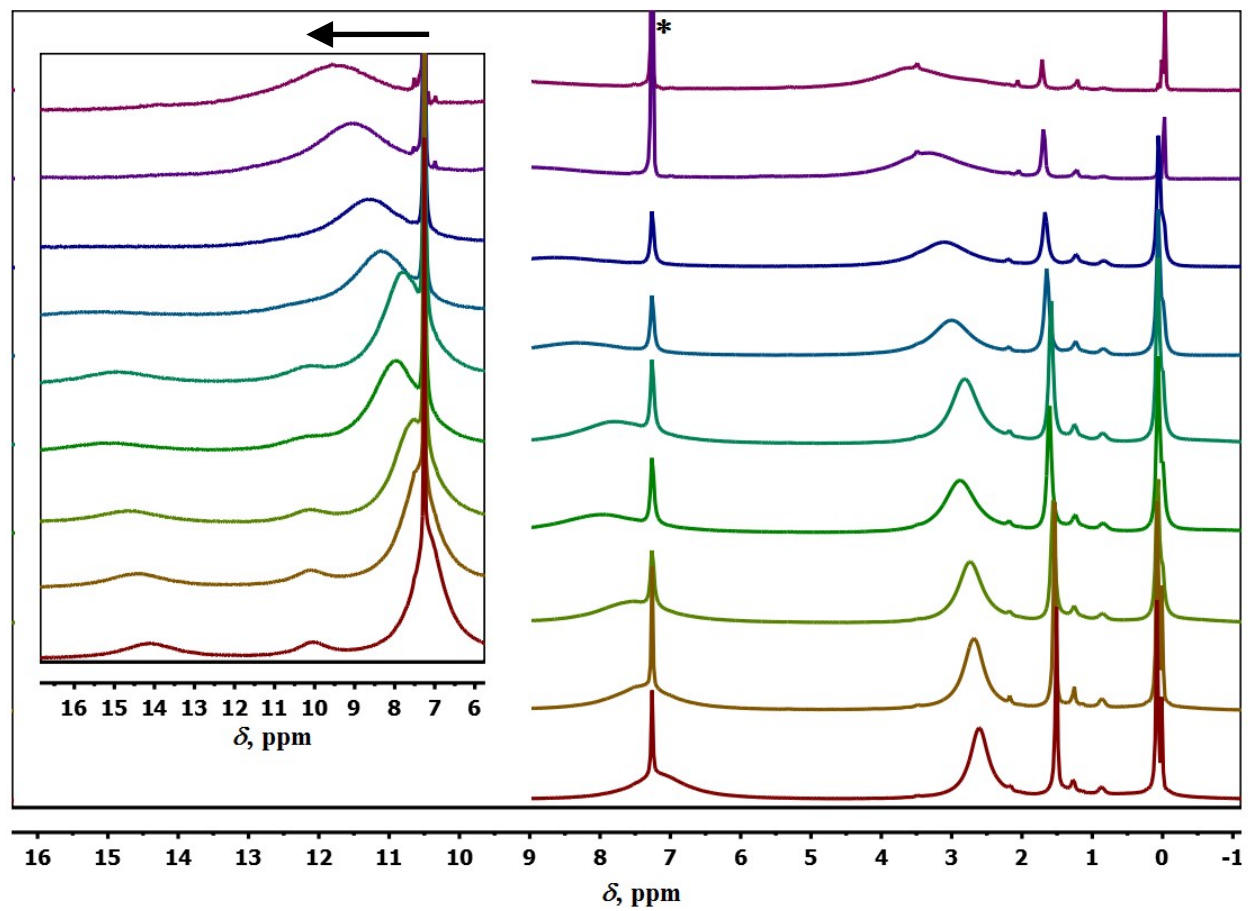


Fig. S12 Variable Temperature (233-313 K) ^1H NMR spectrum (400 MHz, CDCl_3) of $[\text{Co}(\text{L}^1)_2]$ **1**.

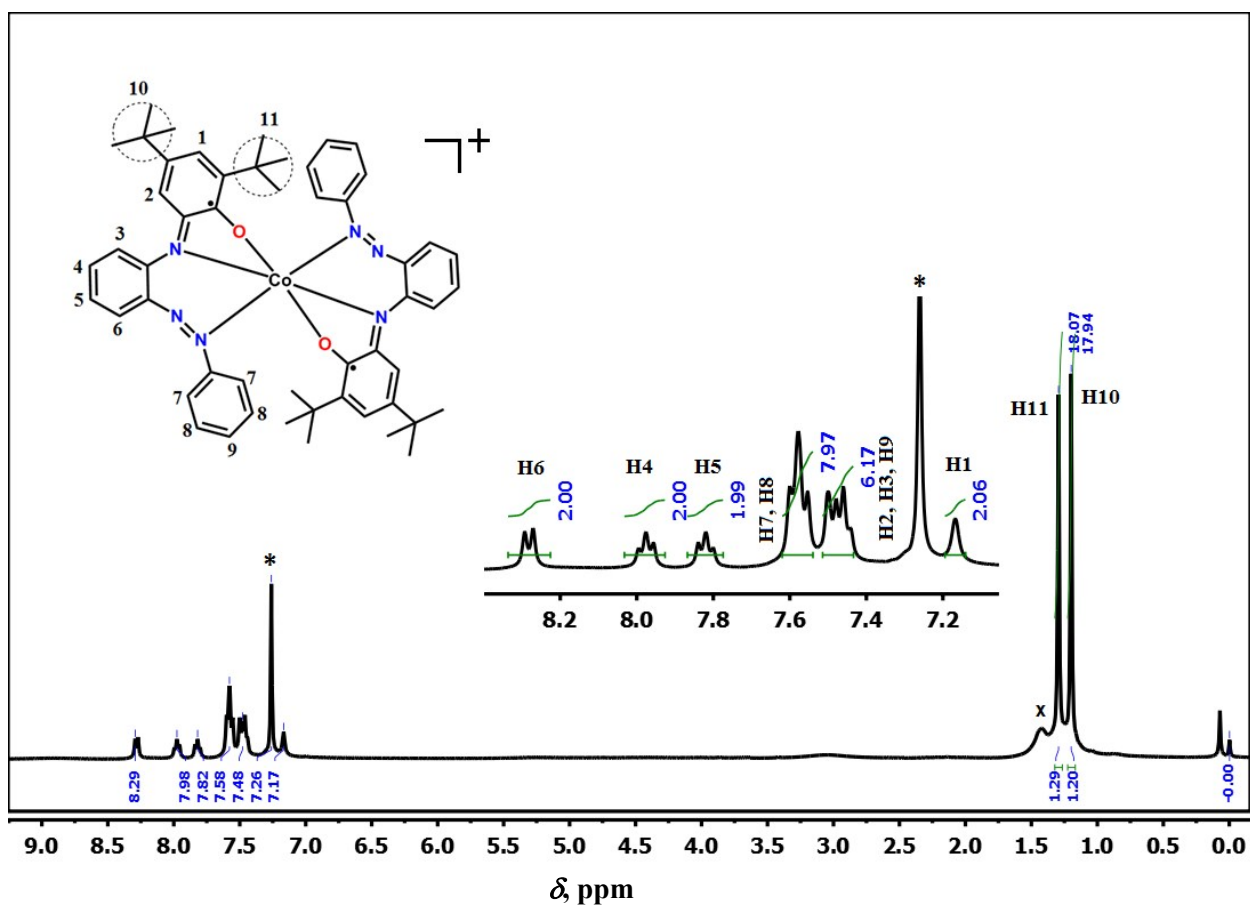
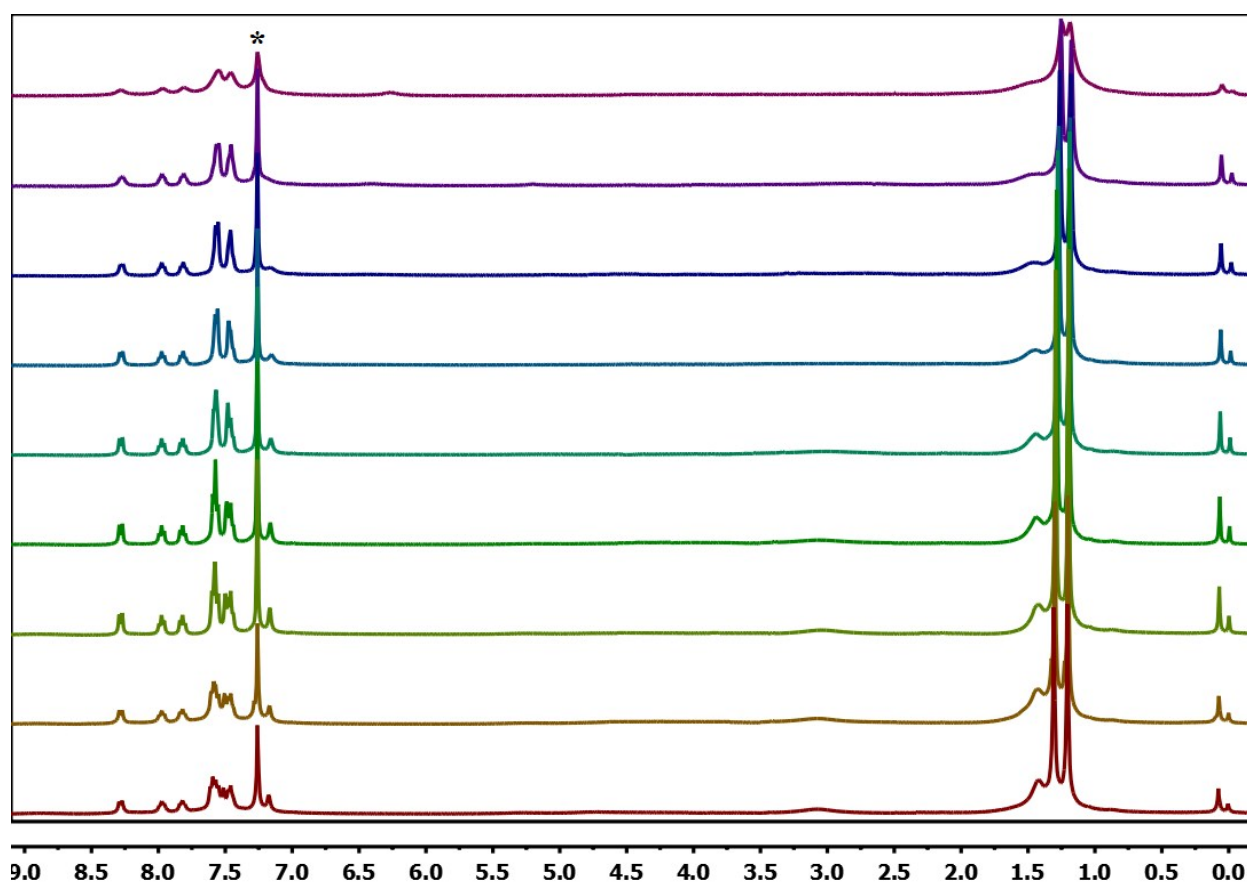


Fig. S13 ^1H NMR spectrum (400 MHz, CDCl_3) of $[\text{Co}(\text{L}^1)_2][\text{PF}_6] \cdot 2\text{CH}_2\text{Cl}_2$ 2 at 298 K. Peaks denoted by * and x are due to CHCl_3 and H_2O respectively.



233 K

273 K

313 K

δ , ppm

Fig. S14 Variable Temperature (233-313 K) ^1H NMR spectrum (400 MHz, CDCl_3) of $[\text{Co}(\text{L}^1)_2][\text{PF}_6]\cdot 2\text{CH}_2\text{Cl}_2$ **2**.

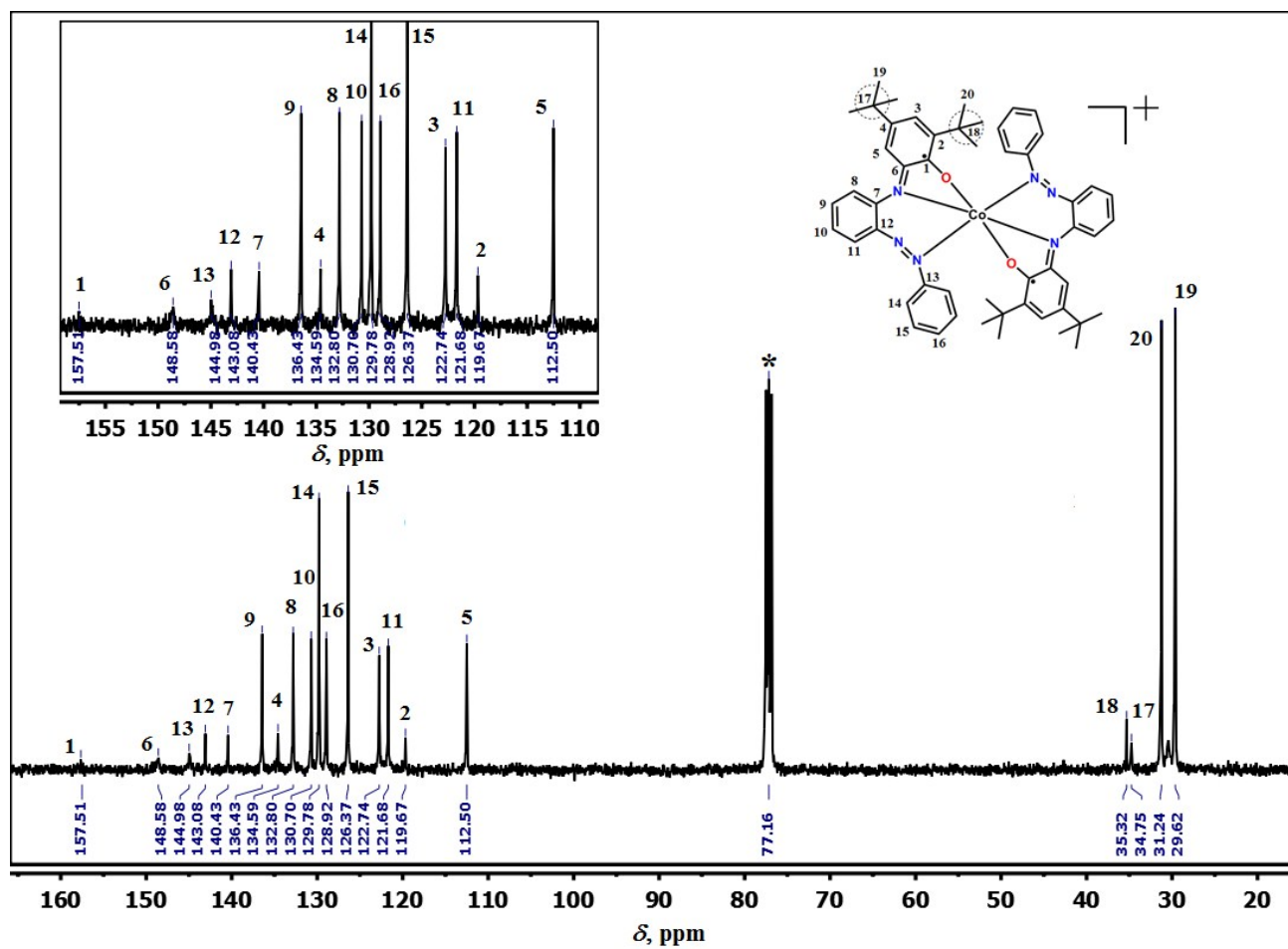


Fig. S15 ^{13}C NMR spectrum (400 MHz, CDCl_3) of $[\text{Co}(\text{L}^1)_2][\text{PF}_6]_2 \cdot 2\text{CH}_2\text{Cl}_2$ **2** at 298 K. Peak denoted by * is due to CHCl_3 .

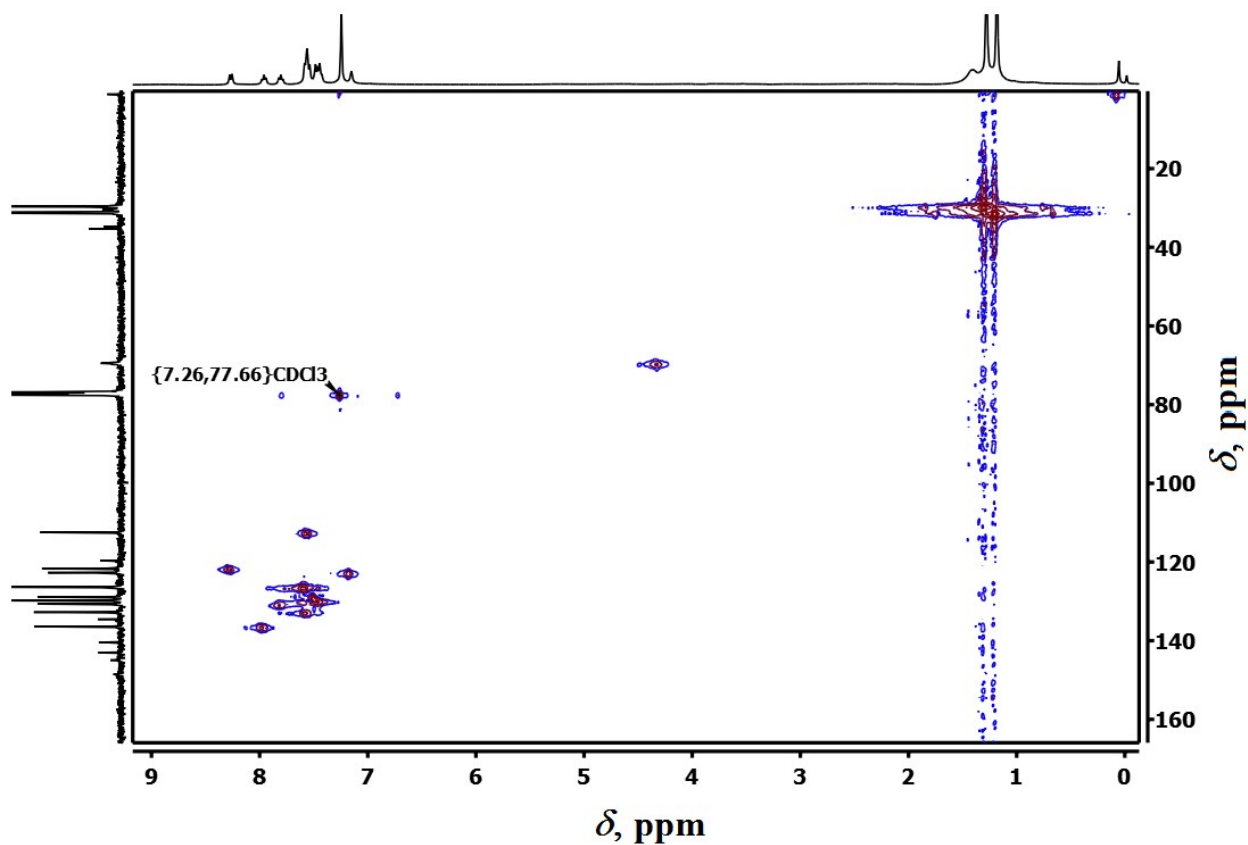
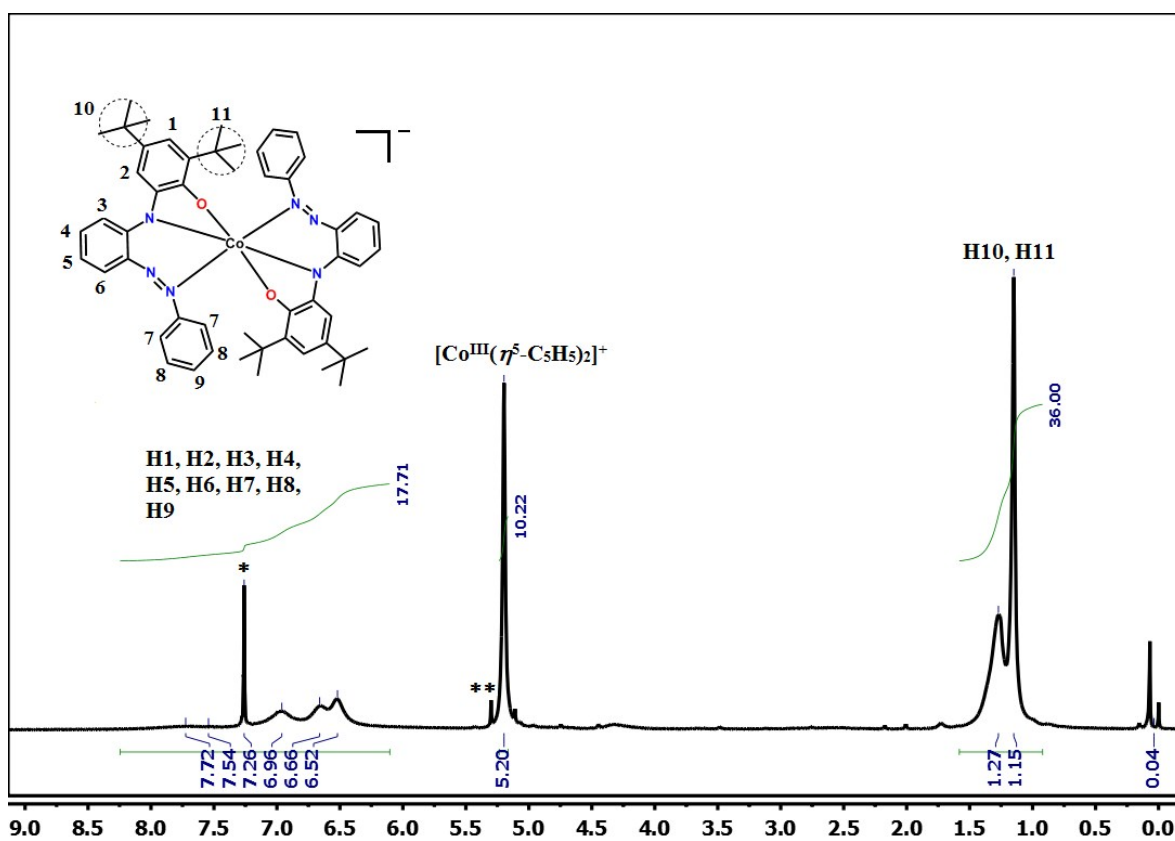
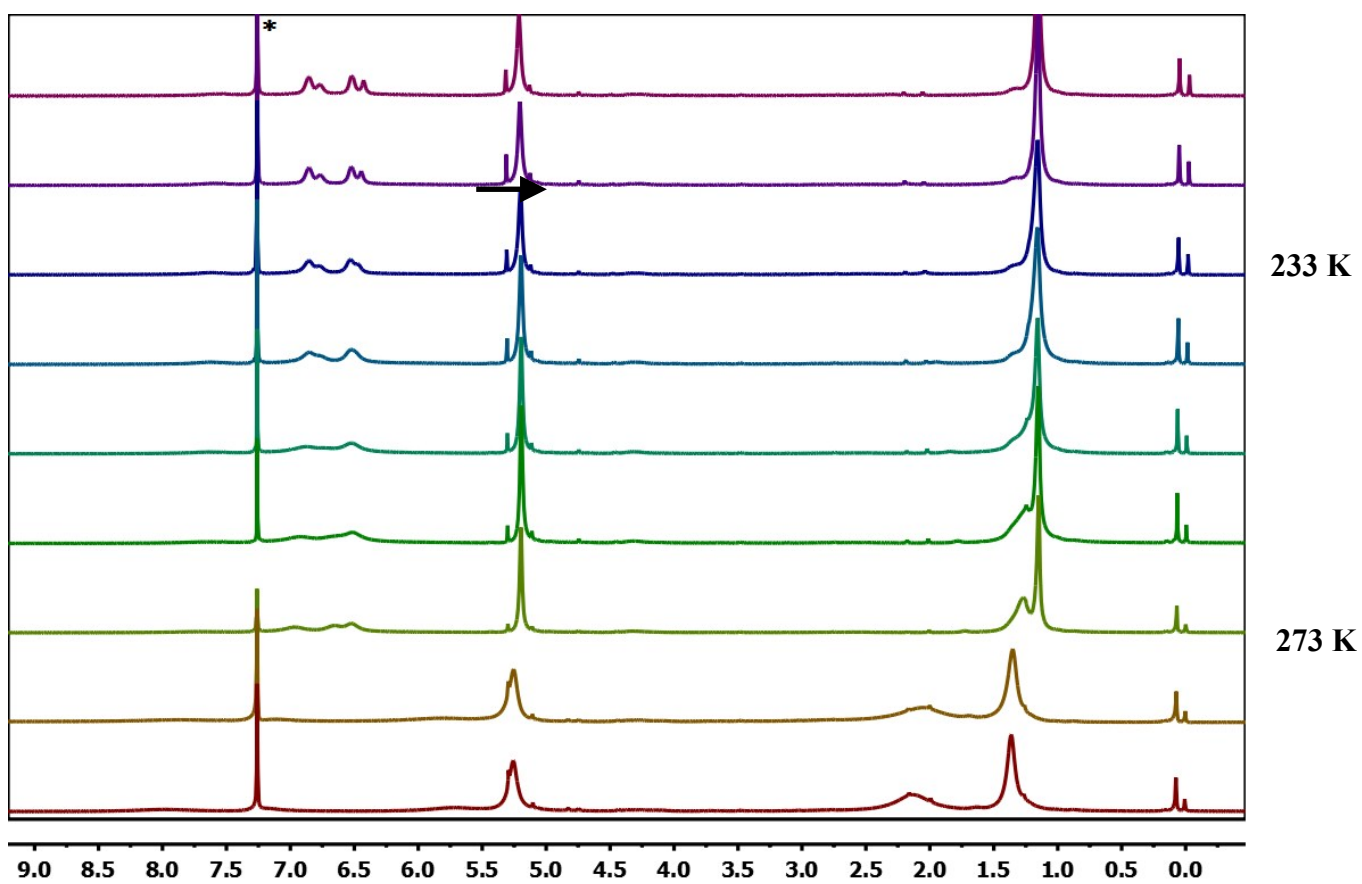


Fig. S16 2D HMQC (Heteronuclear Multiple Quantum Coherence) of (400 MHz, CDCl₃) [Co(L¹)₂][PF₆]₂·2CH₂Cl₂ **2**.



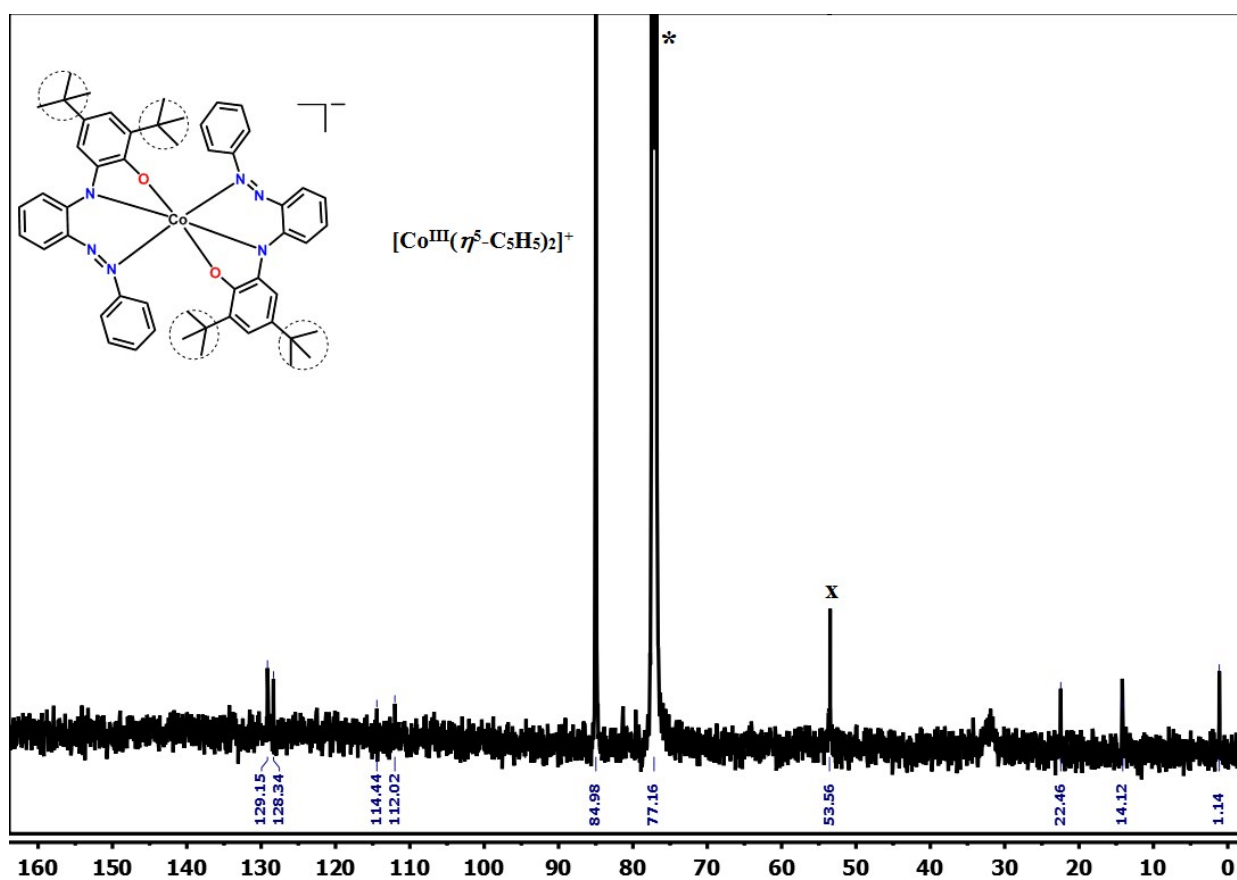
δ , ppm

Fig. S17 ^1H NMR spectrum (400 MHz, CDCl_3) of $[\text{Co}^{\text{III}}(\eta^5\text{-C}_5\text{H}_5)_2][\text{Co}(\text{L}^1)_2]$ **3** 298 K. Peaks denoted by * and ** are due to CHCl_3 and CH_2Cl_2 , respectively



δ , ppm

Fig. S18 Variable Temperature (233-313 K) ^1H NMR spectrum (400 MHz, CDCl_3) of $[\text{Co}^{\text{III}}(\eta^5\text{-C}_5\text{H}_5)_2][\text{Co}(\text{L}^1)_2]$ **3**.



δ , ppm

Fig. S19 ^{13}C NMR spectrum (400 MHz, CDCl_3) of $[\text{Co}^{\text{III}}(\eta^5\text{-C}_5\text{H}_5)_2][\text{Co}(\text{L}^1)_2]$ **3** 298 K. Peaks denoted by * and x are due to CHCl_3 and CH_2Cl_2 .

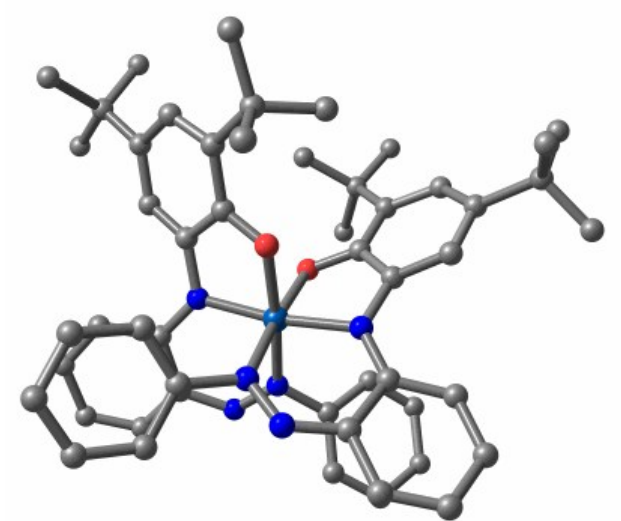


Fig. S20. Optimized-structure for $[1]^{1-}$, where no spin-population is found.

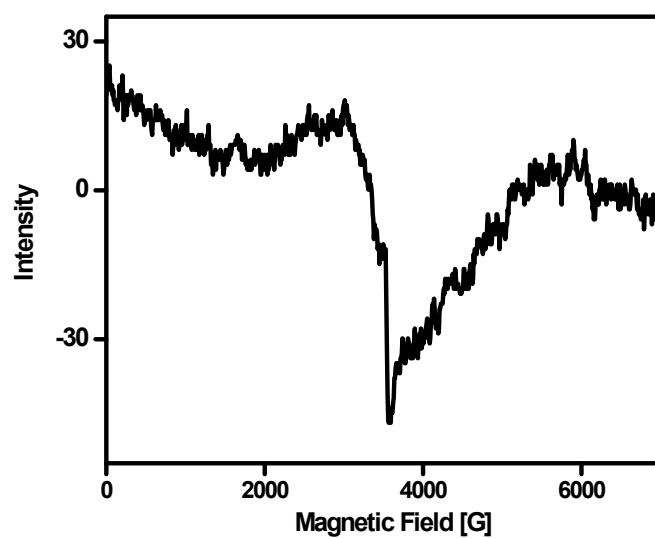
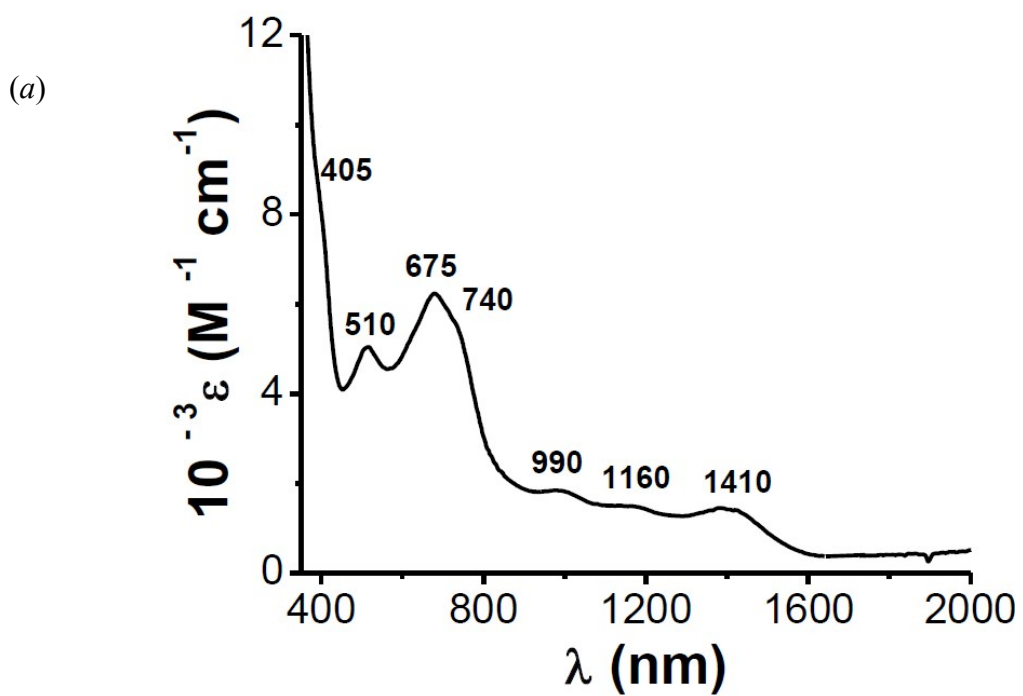


Fig. S21 X-band EPR spectra recorded for $[\text{Co}^{\text{III}}(\eta^5\text{-C}_5\text{H}_5)_2][\text{Co}(\text{L}^1)_2]\text{MeCN}$ **3** as solid (298 K); $g_{\text{iso}} = 2.0053$.



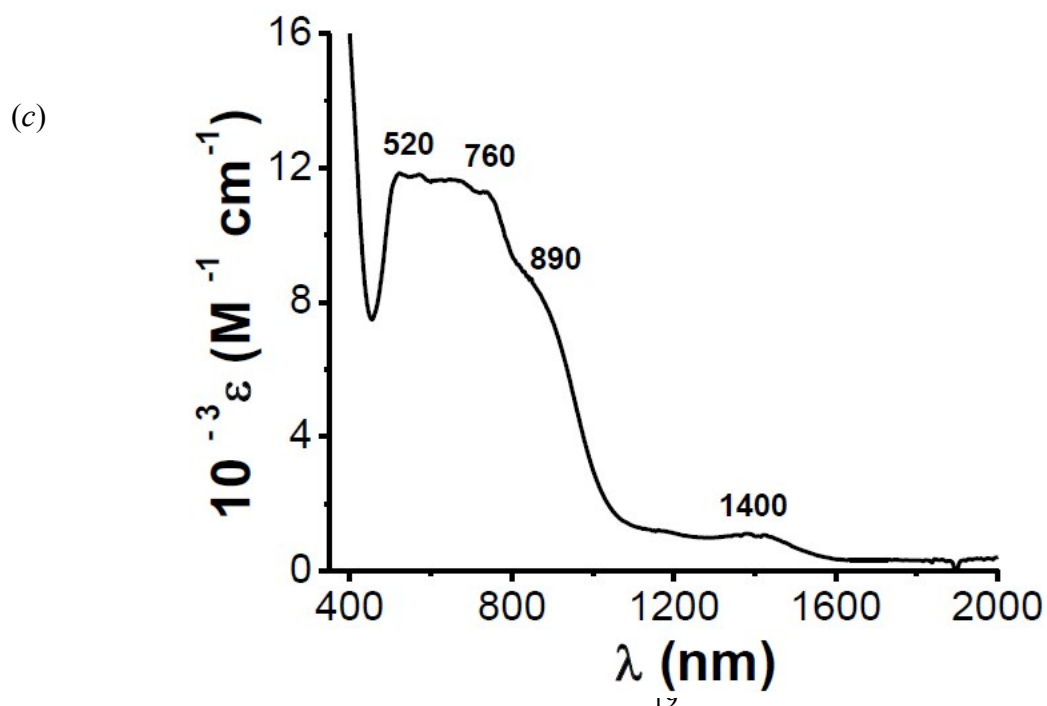
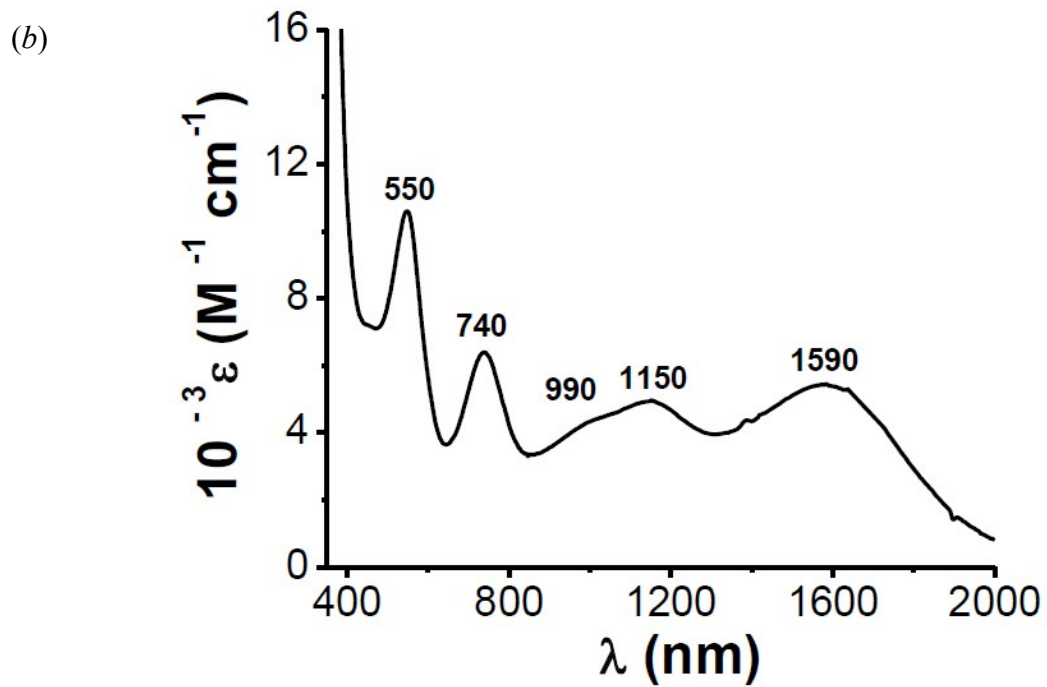


Fig. S22. UV-VIS-NIR spectra of (a) $[\text{Co}(\text{L}^1)_2]$ **1**, (b) $[\text{Co}(\text{L}^1)_2][\text{PF}_6] \cdot 2\text{CH}_2\text{Cl}_2$ **2** and (c) $[\text{Co}^{\text{III}}(\eta^5\text{-C}_5\text{H}_5)_2][\text{Co}(\text{L}^1)_2] \cdot \text{MeCN}$ **3** in CH_2Cl_2 .

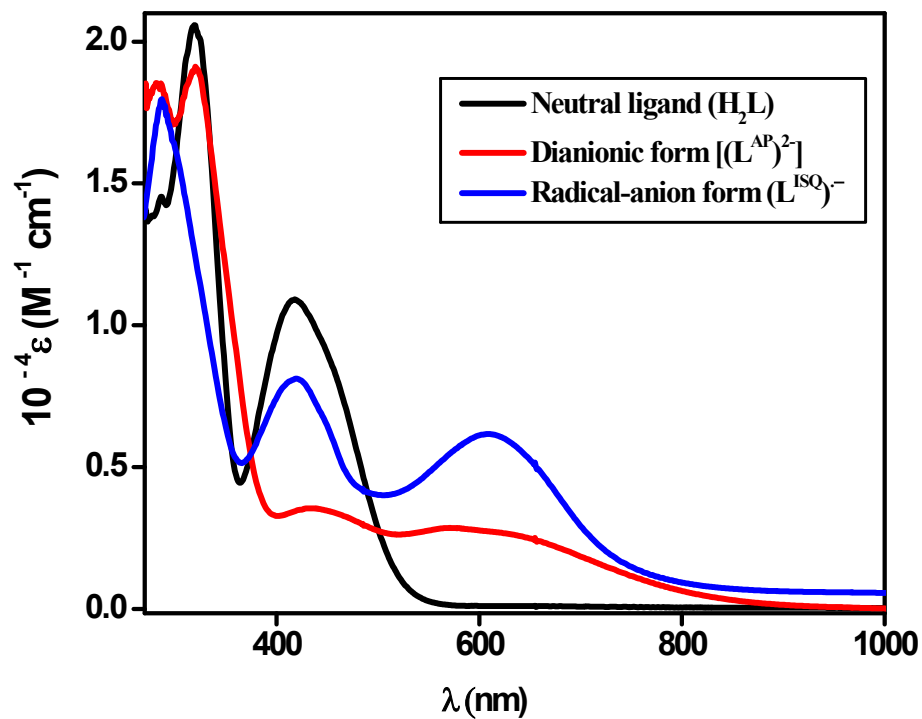
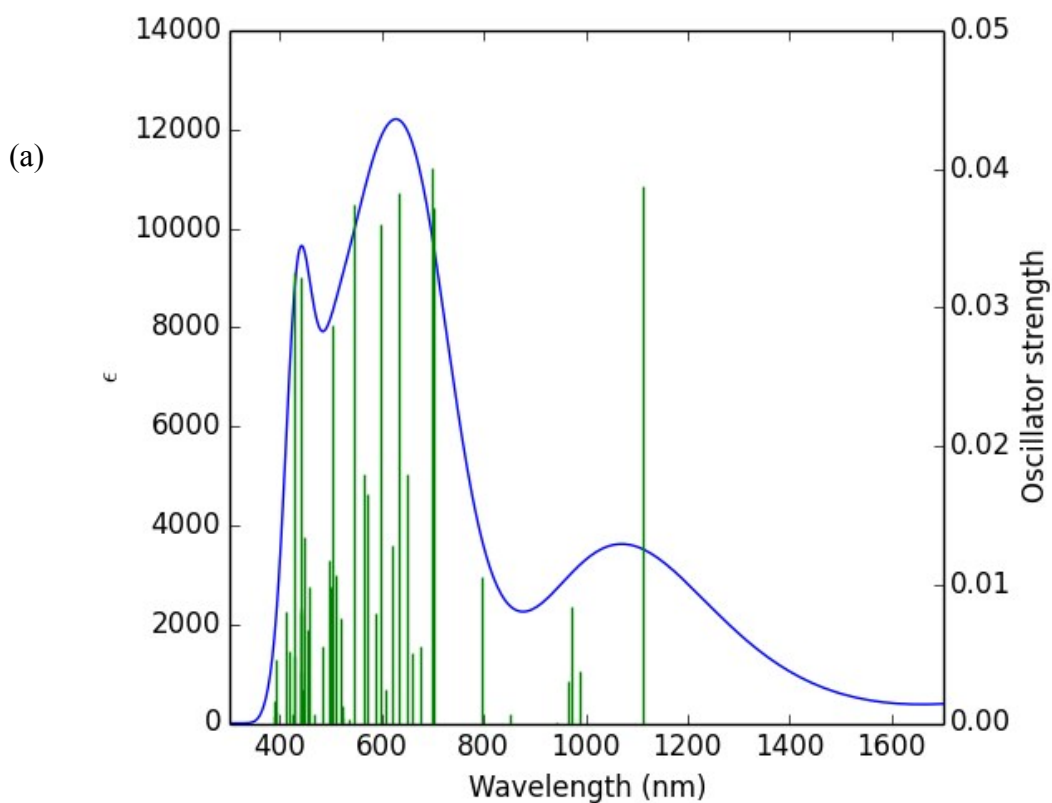


Fig. S23 Absorption spectral measurements on ligand in neutral, dianionic and radical-anion forms recorded in CH_2Cl_2 .



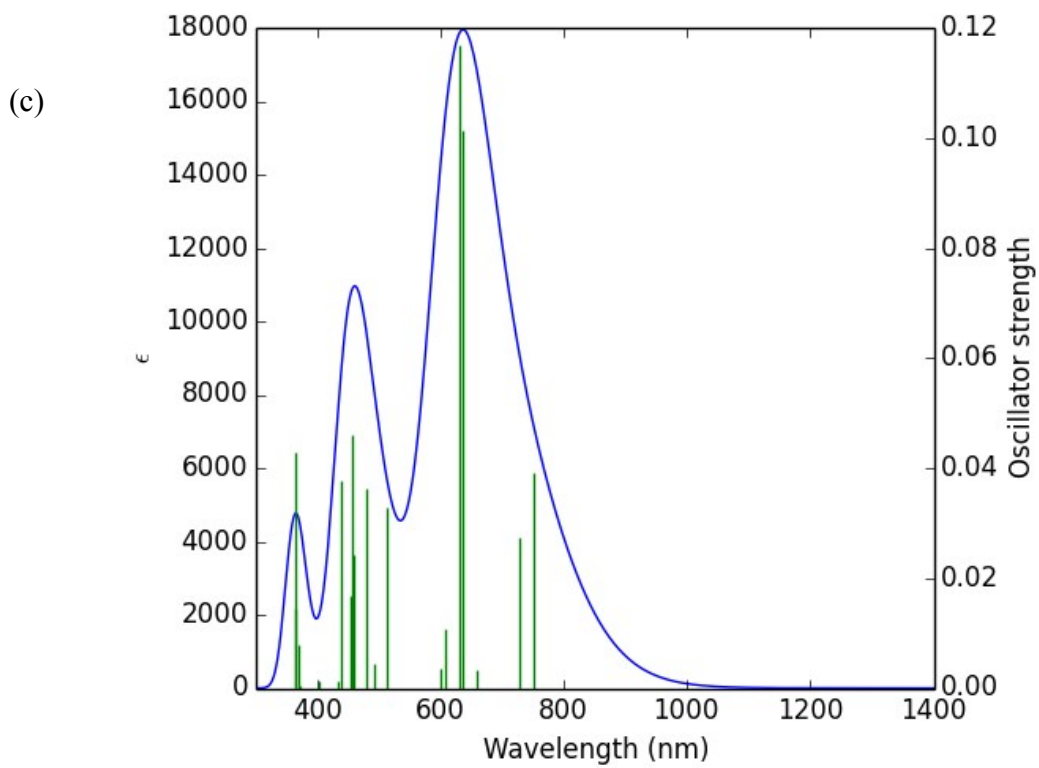
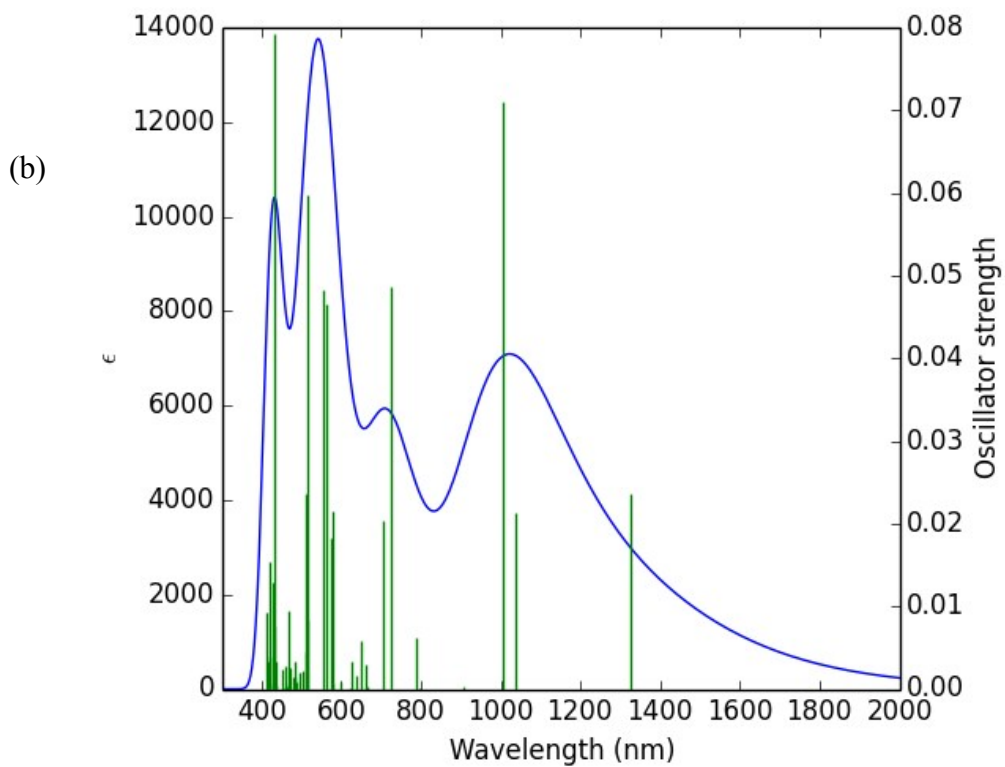
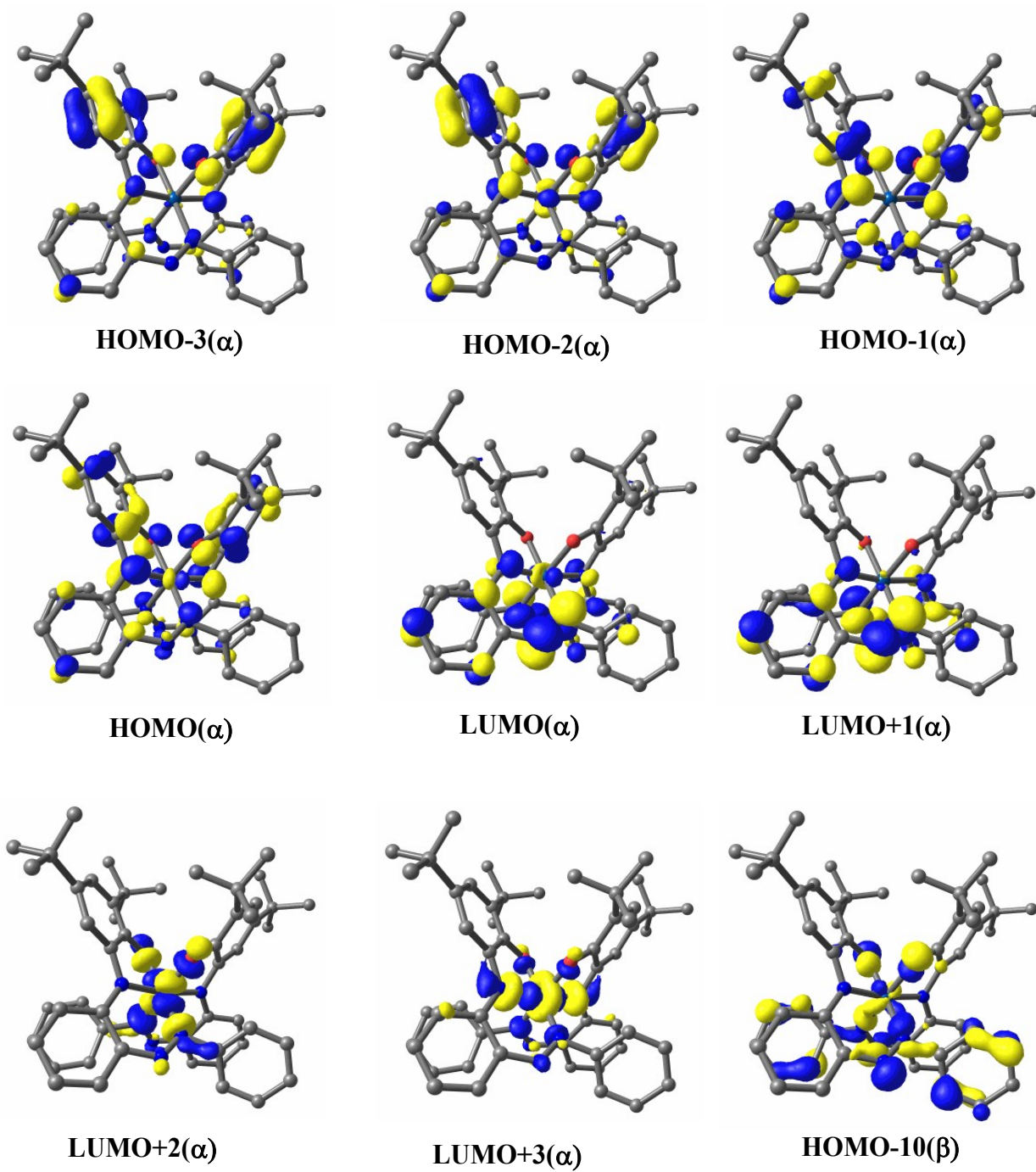


Fig. S24 TD-DFT-Calculated electronic spectra of (a) **1**, (b) $[1]^{1+}$, and (c) $[1]^{1-}$.



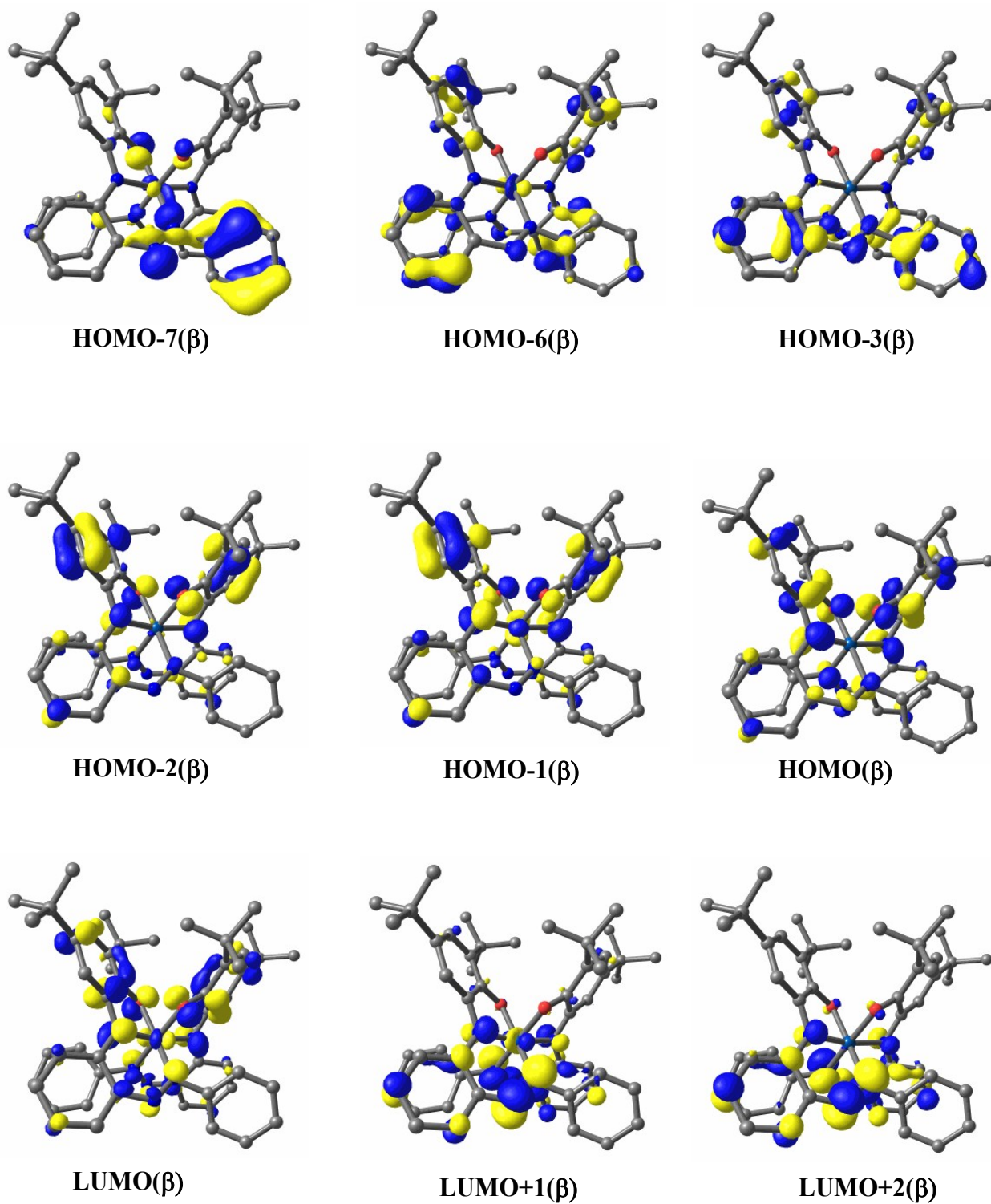


Fig. S25 Representative molecular-orbitals involved in TD-DFT transitions of 1.

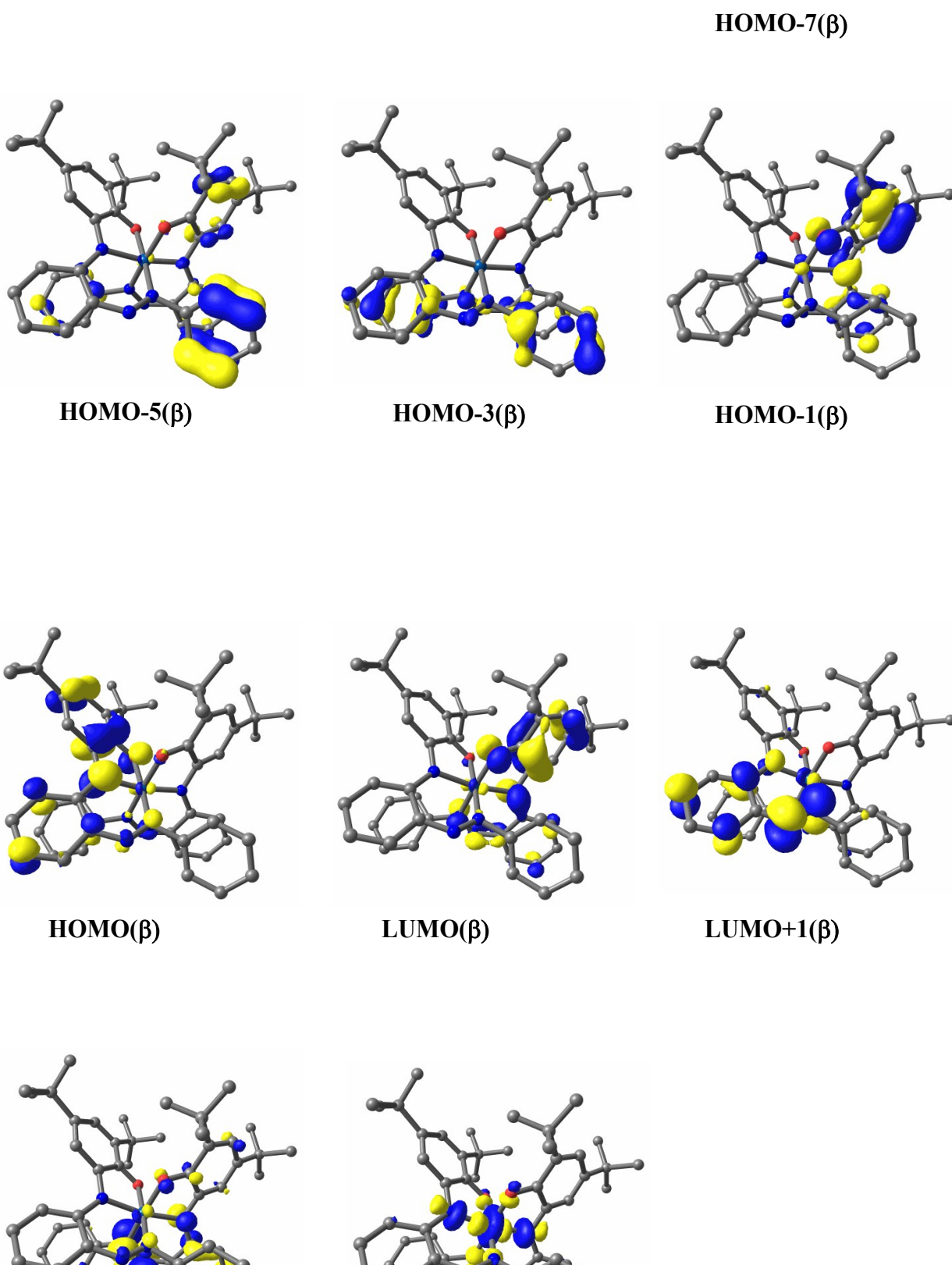


Fig. S26 Representative molecular-orbitals involved in TD-DFT transitions of $[1]^{1+}$.

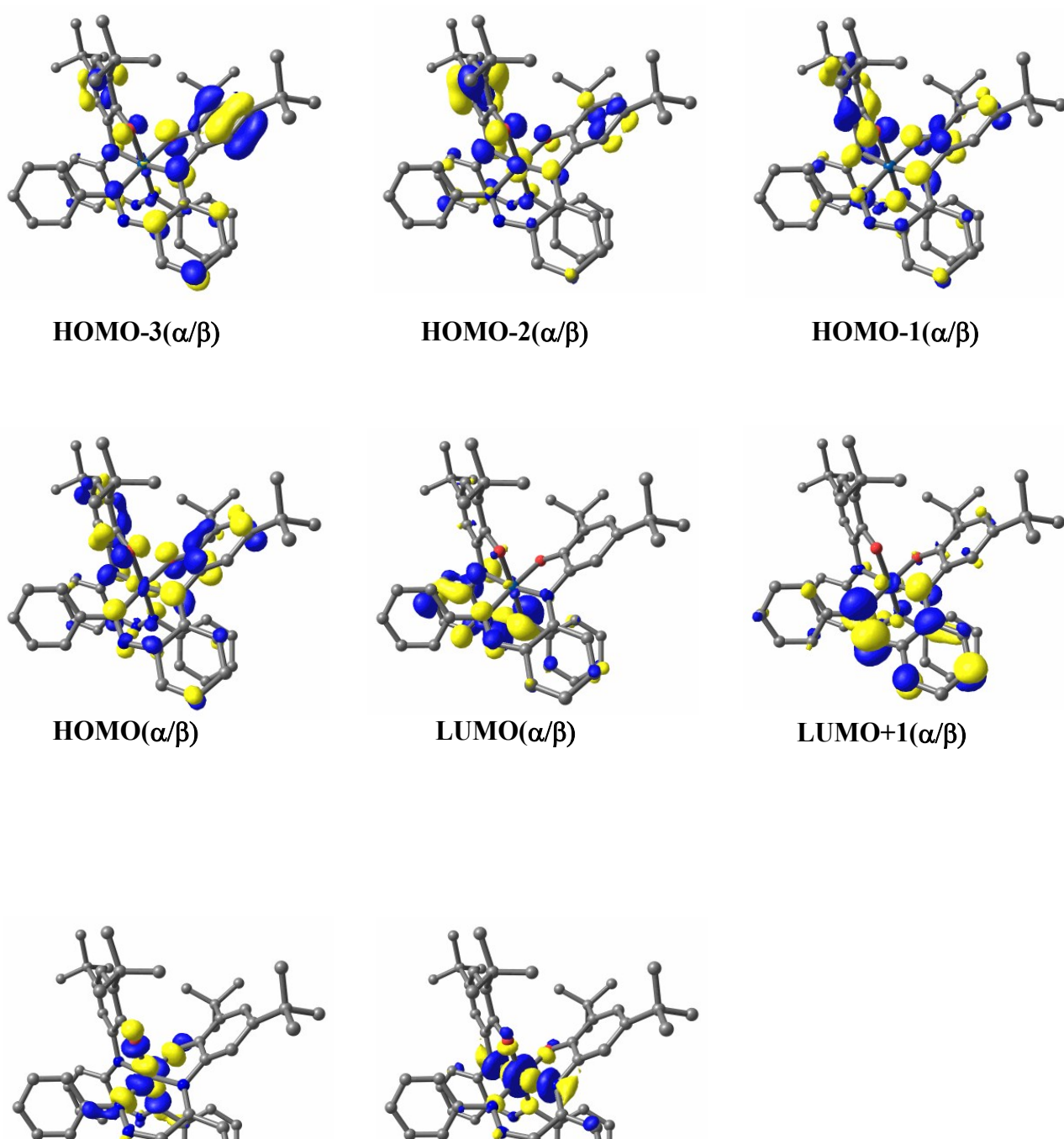


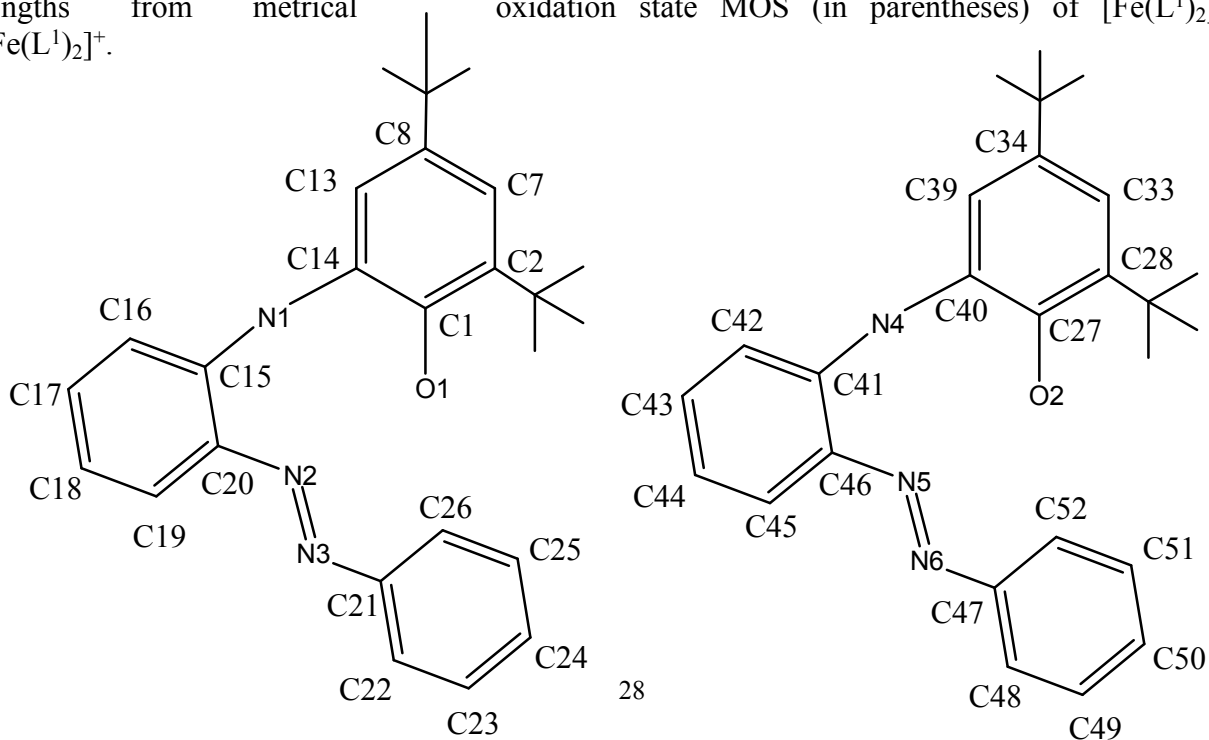
Fig. S27 Representative molecular-orbitals involved in TD-DFT transitions of [1]¹⁻.

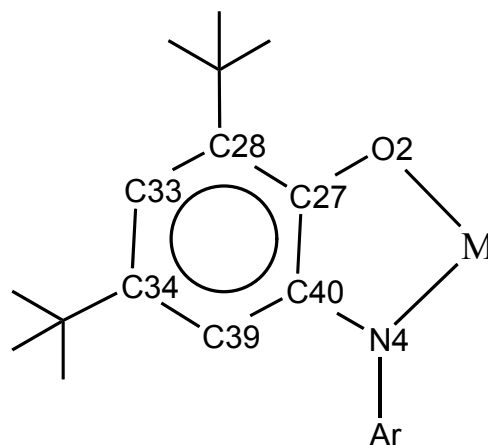
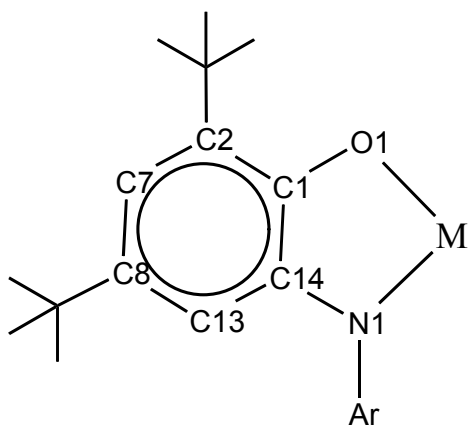
Table S1. Data collection and structure refinement parameters for [Co(L¹)₂] **1**, [Co(L¹)₂][PF₆]₂·2CH₂Cl₂ **2** and [Co^{III}(η⁵-C₅H₅)₂][Co(L¹)₂]₂·MeCN **3**.

	1	2	3
Empirical formula	C ₅₂ H ₅₈ CoN ₆ O ₂	C ₅₄ H ₆₂ Cl ₄ CoF ₆ N ₆ O ₂ P	C ₆₄ H ₇₁ Co ₂ N ₇ O ₂
Formula weight	857.97	1172.80	1088.13
Crystal color, habit	black, prism	black, block	black, block
Temperature (K)	100(2)	100(2)	100(2)
Wavelength (Å)	0.71073	0.71073	0.71073
Crystal system	Orthorhombic	Trigonal	Orthorhombic
Space group	<i>Pca</i> 2 ₁	<i>R</i> 3c	<i>Pna</i> 2 ₁
Crystal size (mm ³)	0.10 x 0.08 x 0.06	0.18 x 0.14 x 0.10	0.1 x 0.07 x 0.05
<i>a</i> (Å)	22.556(5)	31.315(5)	22.6297(14)
<i>b</i> (Å)	12.003(2)	31.315(5)	14.1505(9)
<i>c</i> (Å)	16.456(3)	29.732(5)	17.5120(11)
α (°)	90.0	90.0	90.0
β (°)	90.0	90.0	90.0
γ (°)	90.0	120.0	90.0
Volume (Å ³)	4455.1(16)	25250(7)	5607.7(6)
<i>Z</i>	4	18	4
Density _{calc} (g cm ⁻³)	1.28	1.39	1.289
μ (mm ⁻¹)	0.433	0.395	0.642
no. reflns collcd	22478	53813	28318
no. unique reflns	6811(<i>R</i> _{int} = 0.0823)	6646 (<i>R</i> _{int} = 0.1120)	8128(<i>R</i> _{int} = 0.0706)
no. reflns used [<i>I</i> > 2σ(<i>I</i>)]	5683	4223	6689
Goodness-of-fit on <i>F</i> ²	1.021	1.0419	1.011
Final <i>R</i> indices [<i>I</i> > 2σ(<i>I</i>)] ^{a,b}	0.0491 (0.1056)	0.0786 (0.1985)	0.0484(0.1049)
<i>R</i> indices (all data) ^{a,b}	0.0619 (0.1143)	0.1038 (0.2197)	0.0636(0.1125)

$${}^a R_1 = \Sigma ||F_o| - |F_c|| / \Sigma |F_o|. \quad {}^b wR_2 = \{ \Sigma [w (|F_o|^2 - |F_c|^2)^2] / \Sigma [w (|F_o|^2)^2] \}^{1/2}.$$

Table S2. Comparison of X-ray determined experimental bond lengths with the calculated bond lengths from metrical oxidation state MOS (in parentheses) of $[\text{Fe}(\text{L}^1)_2]$ and $[\text{Fe}(\text{L}^1)_2]^+$.





	[Fe(L ¹) ₂]	[Fe(L ¹) ₂] ¹⁺
C1–O1	1.307(6) [1.312]	1.302(9) [1.291]
C1–C2	1.439(7) [1.421]	1.439(10) [1.431]
C2–C7	1.381(8) [1.382]	1.338(8) [1.373]
C7–C8	1.419(9) [1.421]	1.447(10) [1.434]
C8–C13	1.383(7) [1.375]	1.377(10) [1.367]
C13–C14	1.404(7) [1.408]	1.394(10) [1.415]
C1–C14	1.430(7) [1.435]	1.441(10) [1.452]
C14–N1	1.364(6) [1.358]	1.368(9) [1.341]
C27–O2	1.315(6) [1.334]	1.278(9) [1.295]
C27–C28	1.440(7) [1.412]	1.453(10) [1.429]
C28–C33	1.387(7) [1.391]	1.368(11) [1.375]
C33–C34	1.401(8) [1.408]	1.412(10) [1.432]

C34–C39	1.404(7) [1.383]	1.360(10) [1.368]
C39–C40	1.397(7) [1.401]	1.414(10) [1.414]
C27–C40	1.426(7) [1.422]	1.436(10) [1.448]
N1–C40	1.402(6) [1.376]	1.366(9) [1.344]

Table S3. DFT-optimized coordinates for **1**.

C	-1.121540000	2.212832000	-3.764957000
C	-1.845021000	4.489833000	-3.059007000
C	-3.755984000	-1.855935000	-2.969552000
C	-4.219256000	-3.168213000	-2.837037000
C	5.641459000	2.599998000	-2.022656000
C	3.995157000	-3.805024000	-2.310469000
C	-1.166104000	3.195770000	-2.570441000
C	2.619729000	-3.777806000	-2.365033000
C	-2.491157000	-1.497948000	-2.495308000
C	-3.403954000	-4.132080000	-2.235000000
C	0.274867000	3.550803000	-2.134405000
C	4.665727000	-2.751082000	-1.646129000
C	-1.683164000	-2.464959000	-1.889143000
C	-2.135598000	-3.785960000	-1.767318000

C	1.865707000	-2.730615000	-1.764384000
C	-1.926828000	2.555707000	-1.391409000
C	4.496619000	4.692837000	-1.281154000
C	5.004625000	3.308488000	-0.813750000
C	3.972745000	-1.697064000	-1.086911000
C	2.543967000	-1.625875000	-1.122832000
C	-3.024552000	3.169300000	-0.795506000
C	-1.505165000	1.303892000	-0.832036000
C	3.412707000	1.286022000	-0.740240000
C	-5.982940000	3.706083000	-0.142927000
C	6.099435000	3.501083000	0.262069000
C	3.832616000	2.504491000	-0.218549000
C	2.313028000	0.606855000	-0.176296000
C	-3.744962000	2.635750000	0.307627000
C	-2.295033000	0.686978000	0.197247000
C	-4.893241000	3.456055000	0.926407000
C	-3.371718000	1.383982000	0.783704000
C	3.135246000	3.020892000	0.907235000
C	-4.040149000	-1.587077000	1.019764000
C	1.548301000	1.212535000	0.878138000
C	-2.609958000	-1.569232000	1.060099000
C	-5.548124000	2.733873000	2.117424000
C	-4.772482000	-2.633899000	1.541371000
C	2.017491000	2.425272000	1.483971000
C	1.987583000	-3.925273000	1.602438000
C	-4.348591000	4.813845000	1.429191000
C	-1.973977000	-2.720065000	1.662391000
C	1.582735000	-2.596432000	1.787832000
C	3.241924000	-4.338692000	2.052888000
C	-4.142313000	-3.733545000	2.170008000
C	-0.142857000	3.471766000	2.279865000
C	-2.766838000	-3.758690000	2.226481000
C	2.423651000	-1.688936000	2.439267000
C	1.285757000	3.045554000	2.691790000
C	4.090106000	-3.434696000	2.700724000
C	3.674226000	-2.114361000	2.895557000
C	2.014956000	4.292774000	3.228025000
C	1.209131000	2.017222000	3.845641000
H	-0.592235000	2.674293000	-4.614982000
H	-2.139912000	1.959490000	-4.103211000
H	-1.281764000	4.896504000	-3.913545000
H	-0.598044000	1.284236000	-3.502693000
H	-2.878712000	4.314304000	-3.397423000
H	-4.379154000	-1.100235000	-3.454353000
H	4.920748000	2.458340000	-2.842991000
H	-5.211104000	-3.440964000	-3.206049000
H	4.557445000	-4.623168000	-2.764615000
H	2.051841000	-4.562977000	-2.867568000
H	0.829021000	3.989659000	-2.981349000
H	6.473418000	3.205926000	-2.414835000
H	6.050717000	1.613635000	-1.753124000
H	-2.116652000	-0.484143000	-2.618478000

H	-1.864991000	5.269484000	-2.281468000
H	-3.756304000	-5.161006000	-2.127452000
H	5.322985000	5.281924000	-1.712792000
H	5.755398000	-2.773396000	-1.557438000
H	0.822614000	2.665960000	-1.786092000
H	3.714776000	4.586127000	-2.049694000
H	-1.490221000	-4.531516000	-1.300305000
H	3.901678000	0.855142000	-1.610074000
H	0.264288000	4.291093000	-1.318621000
H	-6.402131000	2.754897000	-0.508266000
H	-3.340678000	4.137041000	-1.180813000
H	-5.589553000	4.254207000	-1.012426000
H	6.489134000	2.529752000	0.606317000
H	6.943458000	4.081438000	-0.146292000
H	4.519616000	-0.926506000	-0.547884000
H	4.070680000	5.276619000	-0.451032000
H	-6.808848000	4.302132000	0.279719000
H	-4.556972000	-0.778622000	0.507209000
H	5.721766000	4.041475000	1.143302000
H	-5.986980000	1.767681000	1.822813000
H	1.316787000	-4.623642000	1.099658000
H	3.487081000	3.961308000	1.327549000
H	-3.908409000	5.408514000	0.614378000
H	-3.879907000	0.938324000	1.634901000
H	-5.862017000	-2.613450000	1.450640000
H	-0.108821000	4.239987000	1.491015000
H	-6.361163000	3.352986000	2.528266000
H	3.557469000	-5.373206000	1.896036000
H	-5.159327000	5.412572000	1.876862000
H	-0.727044000	2.622009000	1.904776000
H	-4.829611000	2.549140000	2.931128000
H	2.059639000	5.102797000	2.483193000
H	-3.569562000	4.666954000	2.193896000
H	-4.734984000	-4.545623000	2.595486000
H	-2.229128000	-4.581070000	2.701985000
H	2.085467000	-0.669223000	2.609901000
H	5.070855000	-3.760264000	3.056350000
H	-0.673940000	3.900712000	3.146360000
H	3.043315000	4.065745000	3.551734000
H	4.323425000	-1.405486000	3.415650000
H	0.649029000	1.120899000	3.548513000
H	1.472106000	4.684592000	4.102507000
H	2.218358000	1.711221000	4.167097000
H	0.701349000	2.463228000	4.716735000
N	0.520691000	-2.856513000	-1.962309000
N	-0.356145000	-2.122631000	-1.420608000
N	1.825808000	-0.634693000	-0.557614000
N	-1.854540000	-0.584876000	0.532019000
N	0.269007000	-2.186080000	1.335678000
N	-0.634497000	-2.903786000	1.854116000
O	-0.437574000	0.661707000	-1.236977000
O	0.457244000	0.595833000	1.259700000

Co	-0.017347000	-0.770747000	-0.016122000
----	--------------	--------------	--------------

Table S4. DFT-optimized coordinates for [1]¹⁺.

C	-0.345095000	0.129397000	0.171504000
C	-0.213429000	0.103497000	2.661692000
C	0.629594000	0.094459000	1.363421000
C	3.775277000	-5.220068000	0.996926000
C	1.442392000	-1.219107000	1.274837000
C	1.024661000	4.890962000	-1.115139000
C	1.590717000	2.239573000	0.332354000
C	1.584448000	1.304358000	1.351241000
C	4.605684000	-5.047990000	2.291820000
C	3.835171000	-5.704989000	3.450360000
C	5.964113000	-5.773703000	2.135950000
C	0.625387000	4.241691000	5.396357000
C	2.433795000	4.261770000	-0.991717000
C	2.729465000	3.405511000	-2.246829000
C	2.477324000	3.366908000	0.257041000
C	1.340619000	3.051085000	5.241190000
C	2.546043000	1.508438000	2.404906000
C	0.988221000	5.163529000	6.383761000
C	4.859174000	-3.552025000	2.538164000
C	4.447096000	-2.900695000	3.686734000
C	5.547681000	-2.792047000	1.532906000
C	3.469224000	5.398286000	-0.927922000
C	3.338607000	3.596659000	1.314650000
C	2.418104000	2.787894000	6.091278000
C	3.356183000	2.715440000	2.424005000
C	5.489282000	0.343823000	-0.196958000
C	2.065027000	4.887460000	7.231776000
C	4.682275000	-1.512161000	3.842431000
C	5.765013000	-1.427302000	1.583453000
C	6.983506000	-1.603953000	-0.648818000
C	5.259932000	-0.747386000	2.749428000
C	2.778828000	3.695215000	7.093671000
C	3.567311000	-0.413110000	7.193032000
C	4.250702000	-1.213429000	6.213937000
C	3.381378000	-0.902076000	8.509642000
C	6.474813000	-0.655882000	0.453546000
C	4.800796000	-2.440781000	6.667052000
C	3.904972000	-2.118800000	8.907650000
C	4.637157000	-2.875401000	7.974696000
C	4.084795000	5.292410000	3.721229000
C	4.605152000	4.014115000	4.052605000
C	4.624481000	6.458135000	4.245885000
C	7.696898000	0.105783000	1.021513000
C	5.680300000	3.983080000	5.006101000

C	5.722787000	6.421798000	5.124195000
C	6.811474000	0.742854000	6.006091000
C	7.560036000	-0.163556000	5.250150000
C	6.235759000	5.191704000	5.493803000
C	6.942516000	0.795339000	7.398345000
C	8.442162000	-1.029200000	5.902578000
C	7.817890000	-0.082483000	8.040879000
C	8.568864000	-0.996155000	7.295089000
H	-1.021390000	-0.736884000	0.228281000
H	-0.972123000	1.034897000	0.173210000
H	-0.916335000	-0.744584000	2.656935000
H	0.176588000	0.070700000	-0.796471000
H	-0.809753000	1.027202000	2.738370000
H	3.584630000	-6.288770000	0.809776000
H	0.757068000	-2.082107000	1.273610000
H	2.802011000	-4.711085000	1.079487000
H	0.234244000	4.131261000	-1.211785000
H	4.292628000	-4.818727000	0.112457000
H	0.414091000	0.014227000	3.558395000
H	0.894749000	2.102137000	-0.492718000
H	0.789598000	5.513444000	-0.237252000
H	2.029283000	-1.255409000	0.343260000
H	0.974882000	5.532849000	-2.009015000
H	5.799382000	-6.847082000	1.951203000
H	2.130540000	-1.332595000	2.122415000
H	-0.231222000	4.441737000	4.748340000
H	3.673254000	-6.771105000	3.230933000
H	2.844987000	-5.246872000	3.599469000
H	1.994228000	2.598564000	-2.385333000
H	1.044166000	2.316894000	4.493866000
H	0.424367000	6.091987000	6.499621000
H	2.699472000	4.036048000	-3.149563000
H	6.553568000	-5.381750000	1.293349000
H	6.573269000	-5.676254000	3.048541000
H	4.389844000	-5.648441000	4.400222000
H	3.905227000	-3.433603000	4.462877000
H	4.627450000	-0.184200000	-0.634893000
H	5.895121000	-3.333388000	0.655398000
H	6.163304000	-2.145702000	-1.145144000
H	3.293423000	6.070806000	-0.073659000
H	3.728493000	2.945774000	-2.186618000
H	3.406737000	6.009135000	-1.841125000
H	5.995077000	0.892682000	-1.007821000
H	5.113334000	1.077840000	0.527279000
H	4.499048000	5.014211000	-0.860215000
H	2.347440000	5.598531000	8.011525000
H	4.038160000	4.427511000	1.291267000
H	2.817846000	-0.270479000	9.198326000
H	7.703696000	-2.342766000	-0.263209000
H	3.208289000	5.354832000	3.079670000
H	7.499262000	-1.016596000	-1.423281000
H	5.408466000	-3.030264000	5.983811000

H	3.764359000	-2.478079000	9.928510000
H	5.096476000	-3.818806000	8.280191000
H	3.612197000	3.464008000	7.759597000
H	4.176234000	7.417374000	3.975211000
H	7.401580000	0.854510000	1.768528000
H	8.222015000	0.630607000	0.207674000
H	8.415611000	-0.589897000	1.484436000
H	7.481043000	-0.165001000	4.164124000
H	6.362233000	1.521875000	7.970088000
H	6.152951000	7.344872000	5.516507000
H	9.045442000	-1.724549000	5.314124000
H	7.078667000	5.108277000	6.181785000
H	7.919095000	-0.044804000	9.127953000
H	9.261352000	-1.675097000	7.797976000
N	2.997503000	0.825452000	7.002079000
N	3.150503000	1.535380000	5.979810000
N	4.400471000	-0.745975000	4.938078000
N	4.093366000	2.843516000	3.567119000
N	5.921112000	1.687784000	5.348791000
N	6.313203000	2.868439000	5.507551000
O	2.708520000	0.677153000	3.385278000
O	5.324488000	0.537577000	2.902202000
Co	4.280202000	1.115898000	4.421215000

Table S5. DFT-optimized coordinates for [1]¹⁻.

Co	16.703954000	7.828361000	10.382383000
O	15.321237000	8.089870000	9.067748000
O	15.387158000	8.208981000	11.733869000
N	18.156827000	7.752652000	11.747968000
N	16.120181000	5.992852000	10.607910000
N	17.005392000	9.730887000	10.157041000
N	18.003375000	7.248078000	8.983920000
C	14.982857000	9.364359000	8.992279000
C	14.507023000	7.227271000	11.819545000
N	19.136026000	8.567194000	11.823247000
C	18.316166000	6.678714000	12.695292000
C	16.883768000	4.916592000	10.414833000
C	14.832509000	5.993983000	11.176462000
C	15.844838000	10.313663000	9.614175000
C	18.177040000	10.344732000	10.325115000
N	18.510835000	6.081853000	8.891556000
C	18.605668000	8.141235000	8.026508000
C	13.819103000	9.825436000	8.306326000
C	13.279445000	7.335468000	12.532763000
C	19.226890000	9.722465000	11.120121000
C	17.270325000	6.340923000	13.563140000
C	19.538605000	5.993833000	12.783273000
C	18.086538000	5.004758000	9.598301000

C	16.633835000	3.629307000	11.014239000
C	13.884441000	4.967966000	11.092711000
C	15.469638000	11.663022000	9.710536000
C	18.523250000	11.605993000	9.717689000
C	17.802098000	8.906963000	7.172876000
C	20.003058000	8.214658000	7.915243000
C	12.916441000	8.837415000	7.537357000
C	13.524679000	11.192937000	8.384667000
C	12.942340000	8.615913000	13.326679000
C	12.388312000	6.250662000	12.462607000
C	20.470325000	10.399633000	11.311693000
H	16.334329000	6.891493000	13.506957000
C	17.449626000	5.324940000	14.505715000
C	19.707157000	4.976347000	13.722657000
H	20.347007000	6.266238000	12.103522000
C	18.887987000	3.842115000	9.383101000
H	15.796711000	3.537485000	11.702734000
C	17.461267000	2.550307000	10.812332000
H	14.117189000	4.085954000	10.495778000
C	12.640745000	5.075966000	11.733408000
C	14.300502000	12.128261000	9.098934000
H	16.094110000	12.335100000	10.294671000
H	17.804921000	12.064065000	9.041367000
C	19.751659000	12.196175000	9.895770000
H	16.720194000	8.827990000	7.249271000
C	18.395959000	9.737933000	6.219096000
H	20.619000000	7.613923000	8.585717000
C	20.587978000	9.053103000	6.966023000
C	12.298902000	7.814134000	8.518699000
C	11.760377000	9.550314000	6.809770000
C	13.747382000	8.088046000	6.468480000
H	12.626467000	11.553283000	7.883577000
C	12.836858000	9.822279000	12.364586000
C	11.605037000	8.497285000	14.083279000
C	14.047384000	8.889884000	14.374451000
H	11.440241000	6.339304000	12.986811000
C	20.747444000	11.608252000	10.722127000
H	21.197055000	9.896745000	11.953464000
C	18.663395000	4.636699000	14.590209000
H	16.628193000	5.075619000	15.182931000
H	20.659623000	4.441090000	13.772866000
H	19.752068000	3.969384000	8.727317000
C	18.601163000	2.633329000	9.968021000
H	17.240728000	1.612495000	11.331926000
C	11.614227000	3.930667000	11.603985000
C	13.841088000	13.598790000	9.184617000
H	19.968382000	13.131957000	9.370927000
C	19.787311000	9.818483000	6.111286000
H	17.758043000	10.324484000	5.552337000
H	21.677901000	9.112867000	6.897885000
H	11.663932000	8.321784000	9.262333000
H	13.076815000	7.259786000	9.059032000

H	11.668864000	7.090512000	7.971876000
H	12.123160000	10.291816000	6.079320000
H	11.082989000	10.064420000	7.510178000
H	11.160277000	8.807429000	6.259139000
H	14.570583000	7.528295000	6.931785000
H	14.171837000	8.794535000	5.735292000
H	13.110132000	7.373764000	5.918691000
H	12.020210000	9.672848000	11.640141000
H	13.768085000	9.965547000	11.801764000
H	12.623412000	10.746396000	12.930627000
H	11.607448000	7.661525000	14.801919000
H	10.751889000	8.357858000	13.400366000
H	11.421850000	9.423933000	14.651918000
H	15.023343000	9.023960000	13.889508000
H	14.122858000	8.054730000	15.091068000
H	13.816410000	9.805633000	14.946185000
H	21.710289000	12.101790000	10.872731000
H	18.795677000	3.838461000	15.325853000
H	19.235601000	1.760216000	9.799413000
C	10.324051000	4.207360000	12.397449000
C	12.224016000	2.612666000	12.136448000
C	11.228717000	3.743959000	10.117615000
C	12.446215000	13.676270000	9.848298000
C	13.761048000	14.206364000	7.764450000
C	14.807217000	14.463131000	10.015304000
H	20.246405000	10.475803000	5.367665000
H	10.523624000	4.326972000	13.474041000
H	9.621887000	3.365170000	12.279896000
H	9.814702000	5.117172000	12.043875000
H	11.505600000	1.779199000	12.042334000
H	12.498251000	2.709557000	13.199471000
H	13.133136000	2.331806000	11.583139000
H	10.502249000	2.920621000	9.998276000
H	12.107120000	3.509119000	9.497489000
H	10.776919000	4.663592000	9.713254000
H	12.099428000	14.722775000	9.915433000
H	12.475284000	13.257180000	10.866566000
H	11.693359000	13.109736000	9.279442000
H	14.746285000	14.179297000	7.271626000
H	13.425524000	15.257861000	7.803876000
H	13.055549000	13.654119000	7.124910000
H	15.820300000	14.477145000	9.583691000
H	14.887022000	14.103271000	11.052798000
H	14.446014000	15.504468000	10.050583000

Table S6. X-Ray structural and DFT-optimized (B3LYP) (in parentheses) selected bond lengths of **[1]**, **[1]¹⁺** and **[1]¹⁻**.

	1	[1]¹⁺	[1]¹⁻
Co–O1	1.911(3) [1.929]	1.926(5) [1.933]	1.922(4) [1.925]
Co–N1	1.887(4) [1.926]	1.886(5) [1.936]	1.894(5) [1.939]
Co–N3	1.920(4) [1.978]	1.927(5) [1.967]	1.930(5) [1.995]
O1–C1	1.327(6) [1.310]	1.286(7) [1.296]	1.343(6) [1.321]
C1–C2	1.423(7) [1.435]	1.427(9) [1.441]	1.405(8) [1.424]
C2–C7	1.381(7) [1.391]	1.385(9) [1.383]	1.395(8) [1.406]
C7–C8	1.401(7) [1.421]	1.403(9) [1.436]	1.390(8) [1.405]
C8–C13	1.389(7) [1.390]	1.381(9) [1.383]	1.373(8) [1.403]
C13–C14	1.397(7) [1.410]	1.404(9) [1.417]	1.389(8) [1.399]
C1–C14	1.416(7) [1.436]	1.422(9) [1.454]	1.402(8) [1.428]
N1–C14	1.403(6) [1.387]	1.402(8) [1.366]	1.416(7) [1.408]
N1–C15	1.345(7) [1.348]	1.349(8) [1.367]	1.336(7) [1.333]
Co–O2	1.908(3) [1.929]	1.922(2) [1.932]	1.921(4) [1.926]
Co–N4	1.891(4) [1.926]	1.873(5) [1.936]	1.888(4) [1.939]
Co–N6	1.918(4) [1.978]	1.946(5) [1.970]	1.930(5) [1.995]
O2–C27	1.316(6) [1.310]	1.301(4) [1.296]	1.337(6) [1.321]
C27–C28	1.434(7) [1.434]	1.429(10) [1.441]	1.408(7) [1.427]
C28–C33	1.387(7) [1.392]	1.355(10) [1.382]	1.390(8) [1.401]
C33–C34	1.410(9) [1.421]	1.438(4) [1.436]	1.399(8) [1.409]
C34–C39	1.374(8) [1.390]	1.367(4) [1.383]	1.386(8) [1.399]
C39–C40	1.405(7) [1.410]	1.407(4) [1.417]	1.391(7) [1.404]

C27–C40	1.416(7) [1.437]	1.421(4) [1.454]	1.404(8) [1.425]
N4–C40	1.386(6) [1.387]	1.373(8) [1.367]	1.416(7) [1.408]
N4–C41	1.362(6) [1.348]	1.380(8) [1.367]	1.331(7) [1.333]

Table S7. TD-DFT-calculated electronic transitions of **1**.

Excitation energy (eV)	λ (nm)	f	Transition	Character
1.1160	1111	0.0388	β -H - 1 [\sim 94%L] \rightarrow β -L [\sim 96%L] (96%)	Inter-ligand charge-transfer (CT) from amido-phenolate moiety to phenyl-iminosemiquinonate moiety
1.2742	973	0.008	β -H [\sim 99%L] \rightarrow β -L + 1 [\sim 96%L] (10%) β -H - 2 [\sim 99%L] \rightarrow β -L [\sim 96%L] (56%)	CT from amido-phenolate and phenyl-iminosemiquinonate to azo Inter-ligand CT from amido-phenolate moiety to phenyl-iminosemiquinonate moiety
1.5550	797	0.0106	α -H [\sim 96%L] \rightarrow α -L + 3 [\sim 38%M] (29%) β -H [\sim 99%L] \rightarrow β -L + 2 [\sim 99%L] (14%)	CT from amido-phenolate and phenyl-iminosemiquinonate to Co and azo CT from amido-phenolate and phenyl-iminosemiquinonate to azo
1.7664	702	0.0372	α -H [\sim 96%L] \rightarrow α -L [\sim 96%L] (39%) β -H [\sim 99%L] \rightarrow β -L + 2 [\sim 99%L] (22%)	CT from amido-phenolate and phenyl-iminosemiquinonate to azo CT from amido-phenolate and phenyl-iminosemiquinonate to azo
1.7742	699	0.0401	α -H [\sim 96%L] \rightarrow α -L + 1 [\sim 99%L] (61%)	CT from amido-phenolate and phenyl-iminosemiquinonate to azo

			$\beta\text{-H}$ [$\sim 99\%L$] \rightarrow $\beta\text{-L} + 1$ [$\sim 96\%L$] (29%)	CT from amido-phenolate and phenyl- iminosemiquinonate to azo
1.9060	651	0.018	$\alpha\text{-H} - 1$ [$\sim 99\%L$] \rightarrow $\alpha\text{-L}$ [$\sim 96\%L$] (72%)	CT from amido-phenolate and phenyl- iminosemiquinonate to azo
			$\beta\text{-H}$ [$\sim 99\%L$] \rightarrow $\beta\text{-L} + 1$ [$\sim 96\%L$] (12%)	CT from amido-phenolate and phenyl- iminosemiquinonate to azo
1.9608	632	0.0383	$\alpha\text{-H} - 1$ [$\sim 99\%L$] \rightarrow $\alpha\text{-L} + 1$ [$\sim 99\%L$] (37%)	CT from amido-phenolate and phenyl- iminosemiquinonate to azo
			$\beta\text{-H}$ [$\sim 99\%L$] \rightarrow $\beta\text{-L} + 2$ [$\sim 99\%L$] (16%)	CT from amido-phenolate and phenyl- iminosemiquinonate to azo
2.0744	598	0.036	$\beta\text{-H} - 3$ [$\sim 99\%L$] \rightarrow $\beta\text{-L}$ [$\sim 96\%L$] (68%)	CT from amino-azo-phenyl moiety to phenyl-iminosemiquinonate
2.2678	547	0.0374	$\alpha\text{-H} - 1$ [$\sim 99\%L$] \rightarrow $\alpha\text{-L} + 2$ [$\sim 42\%M$] (78%)	CT from amido-phenolate and phenyl- iminosemiquinonate to Co and azo
2.4577	505	0.0287	$\beta\text{-H} - 6$ [$\sim 95\%L$] \rightarrow $\beta\text{-L}$ [$\sim 96\%L$] (30%)	CT from amino-azo-phenyl moiety to phenyl-iminosemiquinonate
			$\beta\text{-H} - 7$ [$\sim 93\%L$] \rightarrow $\beta\text{-L}$ [$\sim 96\%L$] (37%)	CT from phenyl appended to azo to phenyl-iminosemiquinonate
2.7999	443	0.0322	$\alpha\text{-H} - 2$ [$\sim 94\%L$] \rightarrow $\alpha\text{-L} + 1$ [$\sim 99\%L$] (34%)	CT from amido-phenolate and phenyl- iminosemiquinonate to azo

			β -H - 10 [\sim 93%L] \rightarrow	CT from phenyl azo to phenyl-
			β -L [\sim 96%L] (21%)	iminosemiquinonate
2.8887	429	0.0326	α -H - 3 [\sim 99%L] \rightarrow	CT from amido-phenolate and phenyl-
			α -L [\sim 96%L] (49%)	iminosemiquinonate to azo

Table S8. TD-DFT-calculated electronic transitions of [1]¹⁺.

Excitation energy (eV)	λ (nm)	f	Transition	Character
0.9366	1324	0.0237	α -H [\sim 98%L] \rightarrow α -L [\sim 98%L] (51%)	Inter-ligand CT involving phenyl- iminosemiquinonate part of one ligand to other ligand
			β -H [\sim 98%L] \rightarrow β -L [\sim 98%L] (47%)	Inter-ligand CT involving phenyl- iminosemiquinonate part one ligand to other ligand
1.1962	1037	0.0213	α -H - 1 [\sim 96%L] \rightarrow α -L [\sim 98%L] (48%)	Intra-ligand CT involving phenyl- iminosemiquinonate
			β -H - 1 [\sim 96%L] \rightarrow β -L [\sim 98%L] (48%)	Intra-ligand CT involving phenyl- iminosemiquinonate
1.2324	1006	0.0711	α -H - 1 [\sim 96%L] \rightarrow α -L [\sim 98%L] (46%)	Intra-ligand CT involving phenyl- iminosemiquinonate
			β -H - 1 [\sim 96%L] \rightarrow β -L [\sim 98%L] (46%)	Intra-ligand CT involving phenyl- iminosemiquinonate
1.7109	725	0.0486	α -H [\sim 98%L] \rightarrow α -L + 1 [\sim 96%L] (42%)	Intra-ligand CT from phenyl- iminosemiquinonate to <i>o</i> -amino-azo part of the ligand
			β -H [\sim 98%L] \rightarrow β -L + 1 [\sim 96%L] (39%)	Intra-ligand CT from phenyl- iminosemiquinonate to <i>o</i> -amino-azo part of the ligand

1.7548	707	0.0204	α -H [\sim 98%L] \rightarrow α -L + 1 [\sim 96%L] (29%)	Intra-ligand CT from phenyl- iminosemiquinonate to <i>o</i> -amino-azo part of the ligand
			β -H [\sim 98%L] \rightarrow β -L + 1 [\sim 96%L] (33%)	Intra-ligand CT from phenyl- iminosemiquinonate to <i>o</i> -amino-azo part of the ligand
2.1466	578	0.0216	α -H - 3 [\sim 99%L] \rightarrow α -L [\sim 98%L] (15%)	CT from azo appended phenyl ring to phenyl-iminosemiquinonate
			β -H - 3 [\sim 99%L] \rightarrow β -L [\sim 98%L] (19%)	CT from azo appended phenyl ring to phenyl-iminosemiquinonate
			α -H [\sim 98%L] \rightarrow α -L + 4 [\sim 40%M] (12%)	LMCT involving phenyl- iminosemiquinonate to Co and CT from phenyl-iminosemiquinonate to azo
			β -H [\sim 98%L] \rightarrow β -L + 4 [\sim 60%L] (12%)	LMCT from phenyl-iminosemi- quinonate to Co and CT from phenyl- iminosemiquinonate to azo
2.1993	564	0.0466	α -H [\sim 98%L] \rightarrow α -L + 2 [\sim 98%L] (13%)	CT from iminosemiquinonate of one ligand to azo in other ligand
			β -H [\sim 98%L] \rightarrow β -L + 2 [\sim 98%L] (13%)	CT from iminosemiquinonate of one ligand to azo- in other ligand
			α -H - 3 [\sim 99%L] \rightarrow	CT from azo-appended phenyl ring to

			α -L [\sim 98%L] (14%)	phenyl-iminosemiquinonate
			β -H - 3 [\sim 99%L] \rightarrow β -L [\sim 98%L] (13%)	CT from azo appended phenyl ring to phenyl-iminosemiquinonate
2.2401	554	0.0482	α -H [\sim 98%L] \rightarrow α -L + 2 [\sim 98%L] (31%)	CT from iminosemiquinonate of one ligand to azo in other ligand
			β -H [\sim 98%L] \rightarrow β -L + 2 [\sim 98%L] (32%)	CT from iminosemiquinonate of one ligand to azo- in other ligand
2.4075	515	0.0597	α -H - 5 [\sim 99%L] \rightarrow α -L [\sim 98%L] (12%)	Intraligand CT in iminosemiquinonate part of ligand and interligand charge-transfer from azo appended phenyl to iminosemiquinonate
			β -H - 5 [\sim 99%L] \rightarrow β -L [\sim 98%L] (31%)	Intraligand CT in iminosemiquinonate part of ligand and interligand CT from azo appended phenyl to iminosemiquinonate
			α -H - 7 [\sim 99%L] \rightarrow α -L [\sim 98%L] (7%)	Intraligand CT in phenyl-iminosemiquinonate part of ligand and interligand charge-transfer from azo appended phenyl to iminosemiquinonate
			β -H - 7 [\sim 99%L] \rightarrow	Intraligand CT in phenyl-

			β -L [\sim 98%L] (19%)	iminosemiquinonate part of ligand and interligand CT from azo appended phenyl to iminosemiquinonate
2.8645	433	0.0793	α -H - 8 [\sim 92%L] \rightarrow α -L [\sim 98%L] (11%)	CT from azo-phenyl to phenyl- iminosemiquinonate
			β -H - 8 [\sim 92%L] \rightarrow β -L [\sim 98%L] (10%)	CT from azo-phenyl to phenyl- iminosemiquinonate
			α -H - 1 [\sim 96%L] \rightarrow α -L + 2 [\sim 98%L] (9%)	Intra-ligand CT from phenyl- iminosemiquinonate to <i>o</i> -amino-azo part of the ligand
			β -H - 1 [\sim 96%L] \rightarrow β -L + 2 [\sim 98%L] (7%)	Intra-ligand CT from phenyl- iminosemiquinonate to <i>o</i> -amino-azo part of the ligand

Table S9. TD-DFT-calculated electronic transitions of [1]¹⁻.

Excitation energy (eV)	λ (nm)	F	Transition	Character
1.6513	751	0.0391	α -H [\sim 96%L] \rightarrow α -L [\sim 99%L] (16%)	Intra and inter-ligand CT involving amido-phenolate moiety to azo
			α -H [\sim 96%L] \rightarrow α -L + 1 [\sim 97%L] (27%)	Intra and inter-ligand CT involving amido-phenolate moiety to azo
			β -H [\sim 96%L] \rightarrow β -L [\sim 99%L] (16%)	Intra and inter-ligand CT involving amido-phenolate moiety to azo
			β -H [\sim 96%L] \rightarrow β -L + 1 [\sim 97%L] (27%)	Intra and inter-ligand CT involving amido-phenolate moiety to azo
1.7047	727	0.0273	α -H [\sim 96%L] \rightarrow α -L [\sim 99%L] (29%)	Intra and inter-ligand CT involving amido-phenolate moiety to azo
			α -H [\sim 96%L] \rightarrow α -L + 1 [\sim 97%L] (15%)	Intra and inter-ligand CT involving amido-phenolate moiety to azo
			β -H [\sim 96%L] \rightarrow β -L [\sim 99%L] (29%)	Intra and inter-ligand CT involving amido-phenolate moiety to azo

			$\beta\text{-H} [\sim 96\%L] \rightarrow$ $\beta\text{-L} + 1 [\sim 97\%L]$ (15%)	Intra and inter-ligand CT involving amido-phenolate moiety to azo
1.9526	635	0.1014	$\alpha\text{-H} - 1 [\sim 99\%L] \rightarrow$ $\alpha\text{-L} + 1 [\sim 97\%L]$ (37%)	Intra and inter-ligand CT involving amido-phenolate moiety to azo
			$\beta\text{-H} - 1 [\sim 99\%L] \rightarrow$ $\beta\text{-L} + 1 [\sim 97\%L]$ (37%)	Intra and inter-ligand CT involving amido-phenolate moiety to azo
1.9661	631	0.1168	$\alpha\text{-H} - 1 [\sim 99\%L] \rightarrow$ $\alpha\text{-L} [\sim 99\%L]$ (38%)	Intra and inter-ligand CT involving amido-phenolate moiety to azo
			$\beta\text{-H} - 1 [\sim 99\%L] \rightarrow$ $\beta\text{-L} [\sim 99\%L]$ (38%)	Intra and inter-ligand CT involving amido-phenolate moiety to azo
2.4124	514	0.0328	$\alpha\text{-H} - 1 [\sim 99\%L] \rightarrow$ $\alpha\text{-L} + 2 [\sim 40\%M]$ (47%)	LMCT involving amido-phenolate to Co
			$\beta\text{-H} - 1 [\sim 99\%L] \rightarrow$ $\beta\text{-L} + 2 [\sim 40\%M]$ (47%)	LMCT involving amido-phenolate to Co
2.5815	480	0.0362	$\alpha\text{-H} - 2 [\sim 92\%L] \rightarrow$ $\alpha\text{-L} [\sim 99\%L]$ (41%)	Intra ligand CT involving amido-phenolate moiety to azo
			$\beta\text{-H} - 2 [\sim 92\%L] \rightarrow$ $\beta\text{-L} [\sim 99\%L]$ (41%)	Intra ligand CT involving amido-phenolate moiety to azo
2.6915	461	0.0241	$\alpha\text{-H} - 1 [\sim 99\%L] \rightarrow$	LMCT involving amido-phenolate to

			$\alpha\text{-L} + 3$ [$\sim 37\%M$] (17%)	Co
			$\alpha\text{-H} - 3$ [$\sim 99\%L$] \rightarrow $\alpha\text{-L} + 1$ [$\sim 97\%L$] (19%)	Intra-ligand CT involving amido-phenolate moiety to azo
			$\beta\text{-H} - 1$ [$\sim 99\%L$] \rightarrow $\beta\text{-L} + 3$ [$\sim 37\%M$] (17%)	LMCT involving amido-phenolate to Co
			$\beta\text{-H} - 3$ [$\sim 99\%L$] \rightarrow $\beta\text{-L} + 1$ [$\sim 97\%L$] (19%)	Intra-ligand CT involving amido-phenolate moiety to azo
2.7089	458	0.0459	$\alpha\text{-H} - 1$ [$\sim 99\%L$] \rightarrow $\alpha\text{-L} + 3$ [$\sim 37\%M$] (30%)	LMCT involving amido-phenolate to Co
			$\beta\text{-H} - 1$ [$\sim 99\%L$] \rightarrow $\beta\text{-L} + 3$ [$\sim 37\%M$] (30%)	LMCT involving amido-phenolate to Co
